Atmospheric
Chemistry
and Physics

Hydroxyl radicals in the tropical troposphere over the Suriname rainforest: comparison of measurements with the box model MECCA

D. Kubistin[1], H. Harder[1], M. Martinez[1], M. Rudolf[1], R. Sander[1], H. Bozem[1,*], G. Eerdekens[1,**], H. Fischer[1], C. Gurk[1], T. Klüpfel[1], R. Königstedt[1], U. Parchatka[1], C. L. Schiller[2,***], A. Stickler[1,****], D. Taraborrelli[1], J. Williams[1], and J. Lelieveld[1]

[1]Department of Atmospheric Chemistry, Max Planck Institute for Chemistry, Mainz, Germany
[2]Department of Chemistry, York University, Toronto, Canada
[*]now at: Institute for Atmospheric Physics, Johannes Gutenberg University Mainz, Germany
[**]now at: Interscience Expert Center, Louvain-la-Neuve, Belgium
[***]now at: Environment Canada, Vancouver, Canada
[****]now at: Oeschger Centre for Climate Change Research and Institute for Geography, University of Bern, Switzerland

Abstract. As a major source region of the hydroxyl radical OH, the Tropics largely control the oxidation capacity of the atmosphere on a global scale. However, emissions of hydrocarbons from the tropical rainforest that react rapidly with OH can potentially deplete the amount of OH and thereby reduce the oxidation capacity. The airborne GABRIEL field campaign in equatorial South America (Suriname) in October 2005 investigated the influence of the tropical rainforest on the HO_x budget (HO_x = OH + HO_2). The first observations of OH and HO_2 over a tropical rainforest are compared to steady state concentrations calculated with the atmospheric chemistry box model MECCA. The important precursors and sinks for HO_x chemistry, measured during the campaign, are used as constraining parameters for the simulation of OH and HO_2. Significant underestimations of HO_x are found by the model over land during the afternoon, with mean ratios of observation to model of 12.2 ± 3.5 and 4.1 ± 1.4 for OH and HO_2, respectively. The discrepancy between measurements and simulation results is correlated to the abundance of isoprene. While for low isoprene mixing ratios (above ocean or at altitudes >3 km), observation and simulation agree fairly well, for mixing ratios >200 pptV (< 3 km over the rainforest) the model tends to underestimate the HO_x observations as a function of isoprene.

Box model simulations have been performed with the condensed chemical mechanism of MECCA and with the detailed isoprene reaction scheme of MCM, resulting in similar results for HO_x concentrations. Simulations with constrained HO_2 concentrations show that the conversion from HO_2 to OH in the model is too low. However, by neglecting the isoprene chemistry in the model, observations and simulations agree much better. An OH source similar to the strength of the OH sink via isoprene chemistry is needed in the model to resolve the discrepancy. A possible explanation is that the oxidation of isoprene by OH not only dominates the removal of OH but also produces it in a similar amount. Several additional reactions which directly produce OH have been implemented into the box model, suggesting that upper limits in producing OH are still not able to reproduce the observations (improvement by factors of ≈ 2.4 and ≈ 2 for OH and HO_2, respectively). We determine that OH has to be recycled to 94% instead of the simulated 38% to match the observations, which is most likely to happen in the isoprene degradation process, otherwise additional sources are required.
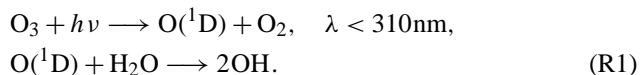
1 Introduction

The hydroxyl radical (OH) and the associated hydroperoxyl radical (HO_2) play a major role in the chemistry of the troposphere, dominating its oxidation capacity during

daytime. Owing to their high chemical reactivity, OH and HO$_2$ are responsible for the removal of most biogenic and anthropogenic trace gases, determining the lifetimes of gaseous pollutants and thereby directly impacting air quality (Heard et al., 2003).

The main source of OH in the unpolluted lower troposphere is the photolysis of ozone, followed by the reaction with water vapour (Levy, 1971):

$$O_3 + h\nu \longrightarrow O(^1D) + O_2, \quad \lambda < 310\,\text{nm},$$
$$O(^1D) + H_2O \longrightarrow 2OH. \tag{R1}$$

Therefore OH production rates are largest in tropical regions, where humidity and radiation intensity are high (Lelieveld et al., 2002).

On the other hand, emissions of biogenic trace gases are controlled by solar radiation and temperature (Kesselmeier et al., 1999; Fuentes et al., 2000). Tropical regions naturally have large areas of rainforest and these ecosystems represent a major source of volatile organic compounds (VOC) on a global scale (Fehsenfeld et al., 1992; Guenther et al., 1995). Global models typically predict a large influence from the tropical rainforest VOC emissions on the hydroxyl radical concentration (Logan et al., 1981; Karl et al., 2007) by the reaction :

$$RH + OH \xrightarrow{O_2} RO_2 + H_2O, \tag{R2}$$

which has been thought to suppress OH and the oxidation capacity of the atmosphere (Wang et al., 1998; Poisson et al., 2000; Lelieveld et al., 2002; Kuhlmann et al., 2004; Joeckel et al., 2006). The main biogenic volatile organic compound (BVOC) emitted from the tropical rainforest is isoprene (Guenther et al., 1995; Granier et al., 2000). Many laboratory based oxidation experiments of isoprene with OH have been performed (e.g., Paulson et al., 1992; Jenkin et al., 1997) and a detailed degradation scheme can be found in Jenkin et al. (1995).

The peroxy radicals generated in the initial step can further react with nitric oxide (NO), forming the hydroperoxyl radical, HO$_2$:

$$RCH_2O_2 + NO \xrightarrow{O_2} RCHO + NO_2 + HO_2, \tag{R3}$$
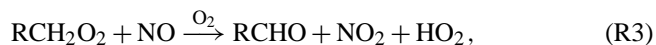
which can recycle OH via reaction with nitric oxide or ozone:

$$HO_2 + NO \longrightarrow OH + NO_2, \tag{R4}$$
$$HO_2 + O_3 \longrightarrow OH + 2O_2. \tag{R5}$$
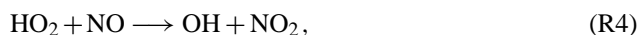
The two radical species OH and HO$_2$ can be considered to be in photochemical equilibrium on a timescale of seconds (Eisele et al., 1994).

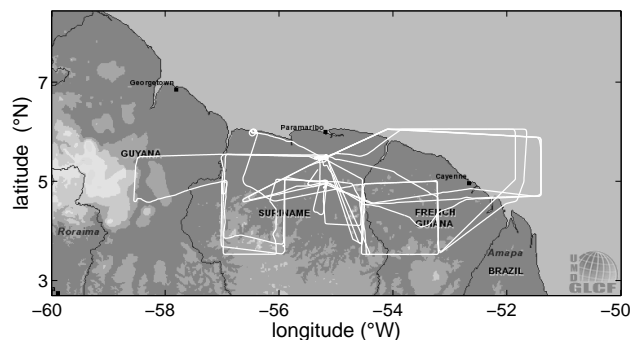**Fig. 1.** Flight tracks over the Guyanas during the GABRIEL campaign (map taken from Earth Science Data Interface (ESDI), University of Maryland).

Table 1. Overview of flights performed during GABRIEL.

Flight	Date	Time of Day
G01	3 Oct 2005	afternoon
G02	5 Oct 2005	noon
G03	6 Oct 2005	afternoon
G04	7 Oct 2005	noon
G05	8 Oct 2005	noon
G06	10 Oct 2005	afternoon
G07	11 Oct 2005	morning
G08	12 Oct 2005	afternoon
G09	13 Oct 2005	afternoon
G10	15 Oct 2005	morning

The objective of the airborne GABRIEL campaign (*G*uyanas *A*tmosphere-*B*iosphere Exchange and *R*adicals *I*ntensive *E*xperiment with the *L*earjet) was to study how the VOC emissions from the pristine rainforest in equatorial South America influence the HO$_x$ (HO$_x$ = OH + HO$_2$) budget. In this study, the impact of BVOCs on the HO$_x$ budget is investigated by comparing the measurements with an observationally constrained box model in steady state. The differences between model and observations for HO$_x$ are analysed and possible modifications of the chemical reaction scheme are discussed.

2 Measurements

The GABRIEL campaign took place over Suriname, French Guiana and Guyana (3° to 6° N, 51° to 59° W). This region is sparsely populated and mainly characterised by pristine rainforest. Flights were performed from Zanderij Airport, Suriname (5° N, 55° W) in October 2005, during the long dry season (August–November). The prevailing wind direction during the campaign was from the tropical Atlantic Ocean towards the rainforest (southeasterly trade winds). The wind
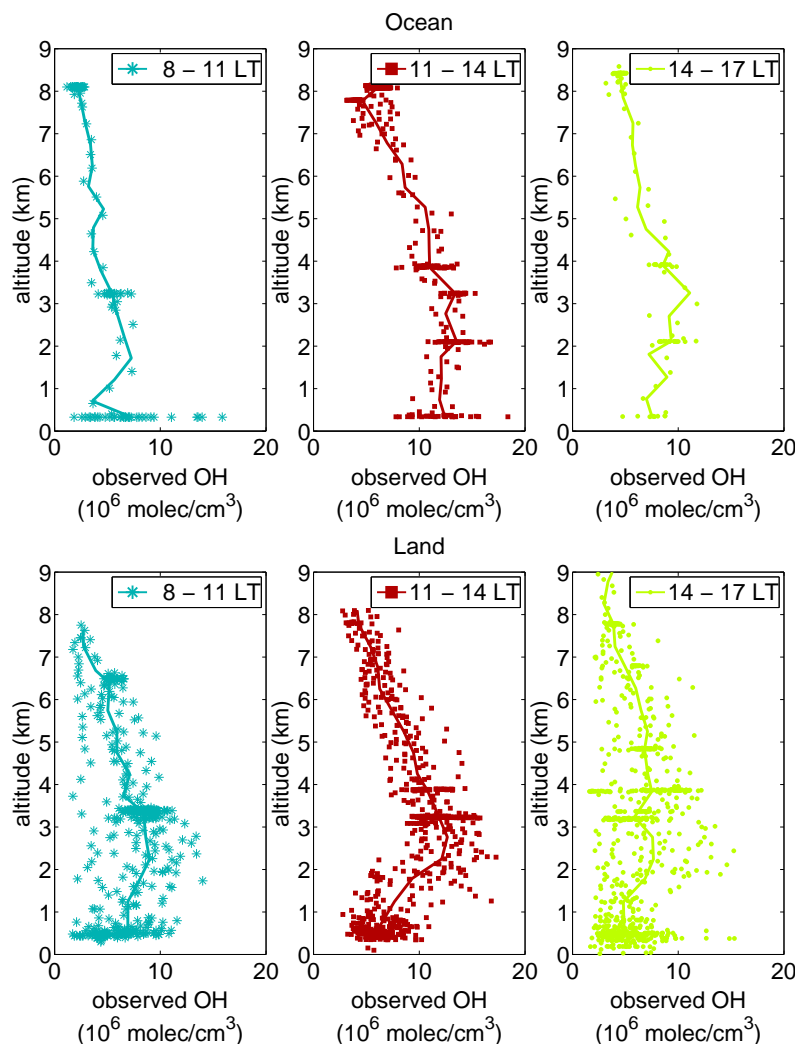
Fig. 2. OH (30 s average) observed for all flights as a function of altitude. The thick line denotes the mean values in 500 m bins. Upper row represents the situation over the ocean for different times of the day (left to right panel), lower row shows the situation over land.

therefore transported clean background maritime air over the forested regions of the Guyanas. Flights were performed to sample air at various altitudes (300 m–9 km) and at different distances from the coast (Fig. 1), hence determining the extent of biogenic influence. The flights were conducted at different times of the day (Table 1), since the primary production of OH in the troposphere is light dependent (R1), as are the emissions of trace gases from the rainforest (Fuentes et al., 2000).

Many important species relevant for fast photochemistry were measured in situ on board a Learjet 35A D-CGFD (GFD[1]). OH was directly detected by the laser induced fluorescence (LIF) technique, whereas HO$_2$ was quantified indirectly by conversion to OH via addition of NO (Martinez et al., 2010). These are the first reported observations of HO$_x$

over the tropical rainforest (Lelieveld et al., 2008). The time resolution of the measurements varied from one to 30 s. An overview of the measured species is given in Table 2.

The measured HO$_x$ data is shown in Figs. 2 and 3. The data (30 s average) was binned in 3-h time intervals to distinguish between morning, noon and afternoon conditions. Local time is UTC (Universal Time Coordinated) minus 3 h. The 1σ uncertainty of the OH and HO$_2$ measurements was estimated to be 20% and 30% by the systematic error and 7% and 1% by the statistical error (as mean value), respectively. A more detailed description can be found in Martinez et al. (2010).

The influence of the rainforest emissions in the boundary layer (<1000 m) is illustrated by the decrease in the OH concentration in the airmass travelling from the ocean to the land. As the VOC accumulate in the atmosphere over the rainforest, they reduce OH and contribute to HO$_2$ production.
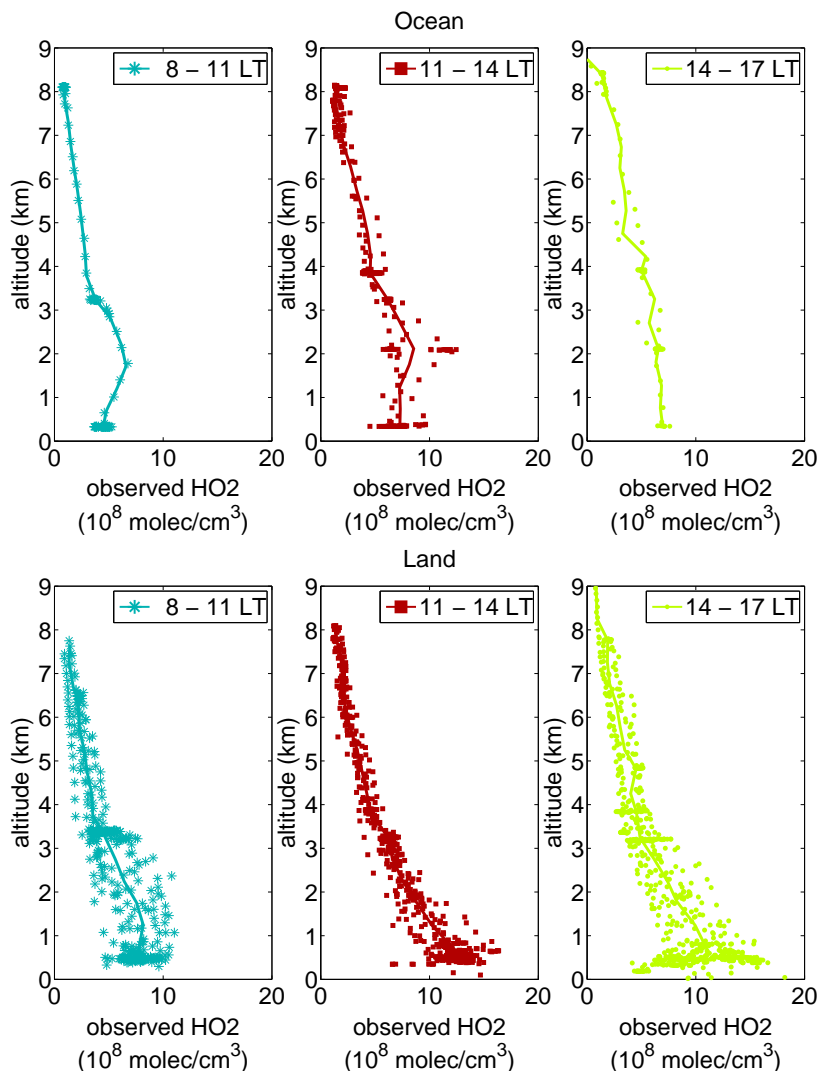

Fig. 3. HO$_2$ (30 s average) observed for all flights as a function of altitude. The thick line denotes the mean values in 500 m bins. Upper row represents the situation over the ocean for different times of the day (left to right panel), lower row shows the situation over land.

To quantify our understanding of the tropospheric chemical processes in more detail, comparisons with box model calculations have been performed. It will be shown that, although OH concentrations decreased over the rainforest, this decrease was much less than expected and possible explanations will be discussed.

3 Box model

The comparison of observed data with chemical box model calculations helps to improve our understanding of the atmospheric oxidation mechanisms. For our analysis, the photochemical box model MECCA (*M*odule *E*fficiently *C*alculating the *C*hemistry of the *A*tmosphere) was used to simulate OH and HO$_2$. The chemical reaction scheme is based on MECCA v0.1p (Sander et al., 2005) containing

the "Mainz Isoprene Mechanism" (MIM) (Poeschl et al., 2000) with 44 reactions and 16 organic species describing the chemistry of isoprene. The maximum number of species in the gas phase is 116 with a total number of 295 reactions. For the simulations, the halogen, sulfur and aqueous phase reactions were neglected and the multiphase chemistry, represented as heterogeneous loss, was only considered in order to represent the deposition of peroxides. The detailed reaction scheme can be found in the accompanying Supplement.

MIM is a reduced reaction scheme in which different species belonging to a class (e.g. carbonyls, peroxy radicals, peroxides and organic nitrates) are lumped into groups of VOC. To verify the influence of the most abundant non methane hydrocarbons (NMHC) over the tropical rainforest, the comprehensive isoprene degradation scheme of the

Table 2. Overview of the species observed and measurement techniques used during the GABRIEL campaign.

Species	Technique	not measured for flight
OH[a]	laser induced fluorescence	G01
HO$_2$[a]	laser induced fluorescence	G01
J(NO$_2$)	filter radiometry	
NO	chemiluminescence	G01, G05, G10
O$_3$	chemiluminescence	G01
HCHO	quantum cascade laser absorption spectroscopy	G02
CO	quantum cascade laser absorption spectroscopy	G02
ROOH[b,c]	derivatisation and fluorimetry	G01, (G05, G07)
H$_2$O$_2$[c]	derivatisation and fluorimetry	G01, G05, G07
Isoprene[d]	proton transfer reaction mass spectrometry	G01, G05
MVK + MACR[e,d]	proton transfer reaction mass spectrometry	G01, G05
Acetone[d]	proton transfer reaction mass spectrometry	G01, G05
Methanol[d]	proton transfer reaction mass spectrometry	G01, G05
H$_2$O	infrared absorption spectrometry (LI-COR)	G02, G07

[a]Martinez et al. (2010), [b]sum of organic peroxides, [c]Stickler et al. (2007), [d]Eerdekens et al. (2008), [e]sum of methylvinylketone and methacrolein

Table 3. Mixing ratios of species which were not measured during the GABRIEL campaign and were fixed for simulation (ppmV $= 10^{-6} \cdot \frac{\text{mol}}{\text{mol}}$, ppbV $= 10^{-9} \cdot \frac{\text{mol}}{\text{mol}}$, pptV $= 10^{-12} \cdot \frac{\text{mol}}{\text{mol}}$). Mixing ratios of alkanes and alkenes were set to zero for altitudes >2 km, except for CH$_4$. Table taken from Stickler et al. (2007).

Species	Mixing ratio ≤ 2 km/ >2 km	Reference
C$_2$H$_4$	(650/0) pptV	GTE ABLE 2A, Manaus, Brazil (Zimmermann et al., 1988)
C$_2$H$_6$	(794/0) pptV	LBA-CLAIRE98 campaign, IMAU (Univ. Utrecht, The Netherlands)
C$_3$H$_6$	(83/0) pptV	LBA-CLAIRE98 campaign, IMAU (Univ. Utrecht, The Netherlands)
C$_3$H$_8$	(83/0) pptV	LBA-CLAIRE98 campaign, IMAU (Univ. Utrecht, The Netherlands)
C$_4$H$_{10}$	(28/0) pptV	LBA-CLAIRE98 campaign, IMAU (Univ. Utrecht, The Netherlands)
CH$_4$	1.7 ppmV	NOAA CMDL Global Trends, ESRL Global Monitoring Division
CO$_2$	377 ppmV	NOAA CMDL Global Trends, ESRL Global Monitoring Division
H$_2$	563 ppbV	Schmidt (1974, 1978)
HNO$_3$	0	

Master Chemical Mechanism MCM 3.1 (Jenkin et al., 1997; Saunders et al., 1997, 2003) was also used in our studies.

The photolysis frequencies (J) were calculated using the radiative transfer model TUV v4.1 (*T*ropospheric *U*ltraviolet-*V*isible Model) (Madronich et al., 1998). The ozone column was determined for every flight from satellite data (GOME, available at: www.knmi.nl) and varied around 265 DU for all flights. The cross sections and quantum yields for the different species were taken from the recommended data of Atkinson et al. (2004, 2005) and Sander et al. (2006). The calculated photolysis frequencies were corrected for cloud and aerosol effects by scaling to the measured J(NO$_2$).

Considering the short lifetimes of OH and HO$_2$ radicals, all model runs were performed to reach steady state. To constrain the model runs, the measured species during the

GABRIEL campaign were fixed to their observed values with a time resolution of 2 min. Trace gases which were not measured were either calculated by the model or taken as fixed parameters as given in Table 3. Although the instruments generally operated steadily and reliably during the GABRIEL campaign, some short interruptions, calibrations or malfunctions did occur. As nitric oxide (NO) is a crucial parameter for the HO$_x$ cycling, datasets without NO data were omitted from this study (flights G01, G05 and G10). For water vapour and carbon monoxide, missing data points were interpolated within 2 min intervals for equal altitude levels. For two flights (G02, G07) water data were not available. As H$_2$O concentration correlates with altitude and the day-to-day variability was small, the mean vertical profile of water from the 8 other flights was used as a proxy to
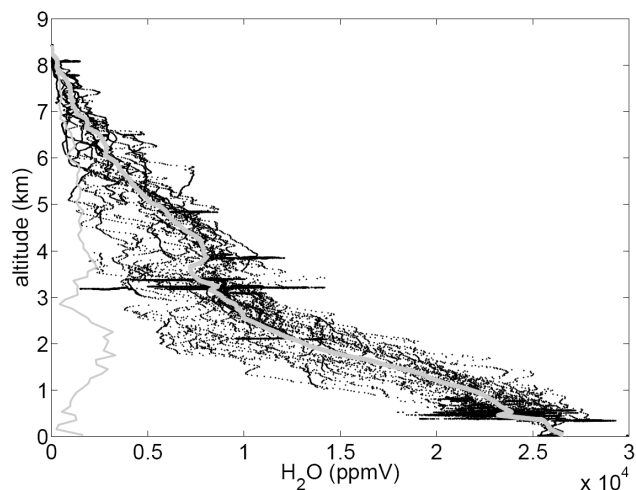
Fig. 4. Observed H$_2$O (1 s resolution) data for all flights as a function of altitude. The thick grey line denotes the mean values for 100 m bins, the thin grey line the standard deviation.
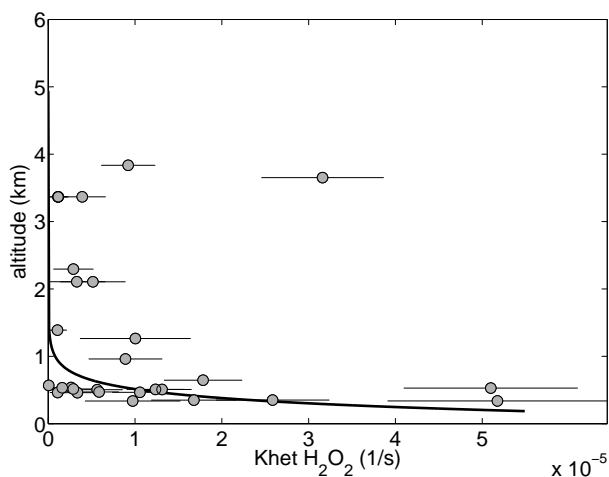

Fig. 5. Calculated heterogeneous removal rate khet(H$_2$O$_2$) as a function of altitude, as caused by wet and dry deposition processes.

Fig. 6. Observed and modelled data for hydrogen peroxide (H$_2$O$_2$ = HOOH) and total organic peroxides (ΣROOH). The solid line represent perfect agreement, the dashed lines bound the 1σ confidence level (1σ-CL).
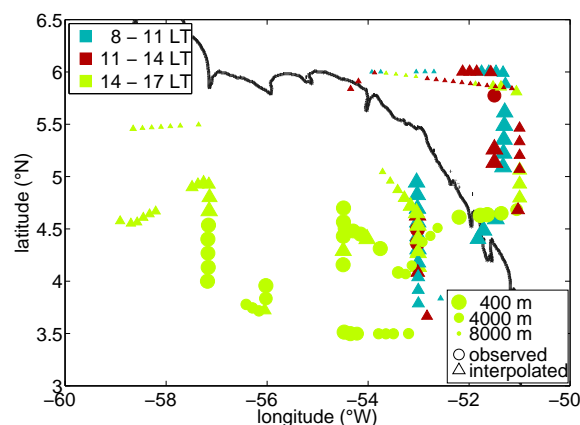
Fig. 7. Measurement locations of data points used to model OH and HO$_2$. The black line represents the coastline.

fill in the missing data. The uncertainty was derived from the standard deviation of the mean profile (Fig. 4). For hydrogen peroxide (H$_2$O$_2$), missing data were simulated by using an altitude dependent heterogeneous removal rate function, which was fitted to loss rates determined by the model to match the measured data where available (Fig. 5). This loss rate is in reasonably good agreement with calculated deposition rates by Stickler et al. (2007), who determined deposition rates in the boundary layer of 1.35×10^{-5} s^{-1} up to 1.35×10^{-4} s^{-1} for the tropical rainforest and about 3.25×10^{-5} s^{-1} for the tropical Atlantic. Total organic peroxides (Σ ROOH) were modelled by using the same removal rates as for H$_2$O$_2$. Comparison of the simulated and measured data shows a slight underestimation of hydrogen
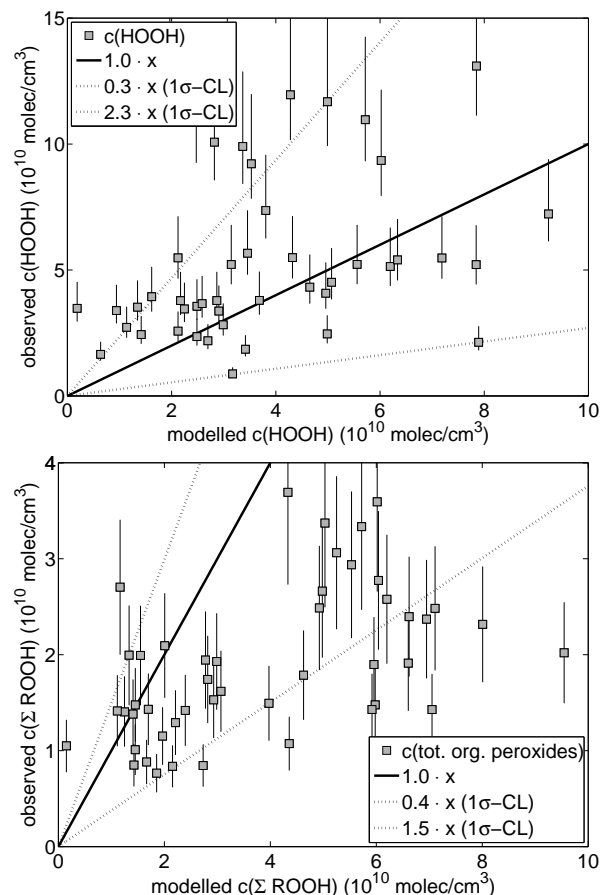
Fig. 8. Ratio of observed to simulated OH and HO$_2$. The black line represents the coastline.

Fig. 9. Error estimates for the simulations due to measurement uncertainties. The solid line represents the perfect match of simulation and observations. The dashed lines correspond to ratios of 1:2 and 2:1. Red points illustrate deviations by more than a factor of $2^{\pm 1}$.

peroxide and overestimation of total organic peroxides (Fig. 6). For altitudes higher than 5.5 km, measurements of total peroxides and H$_2$O$_2$ could not be carried out (Stickler et al., 2007). These missing data were simulated with a removal rate of zero (Jackson and Hewitt, 1999). Altogether, the whole dataset used for the simulation of OH and HO$_2$ consists of 140 data points, corresponding to 280 min of data. The dataset from the direct measurements predominately comprises regions over land in the afternoon at low altitudes (Fig. 7). Datasets for the morning and for high altitudes could only be established based on the assumptions described above and accordingly have a larger uncertainty. Model simulations which used these more uncertain data points are marked separately (triangles). Nevertheless, the overall uncertainty for the modelling of HO$_x$ as caused by these assumptions is less than 50%.

Uncertainties originating from the inaccuracies of the kinetic rate coefficients were estimated by Monte Carlo simulations. Hereby all kinetic rate coefficients were assumed to have an u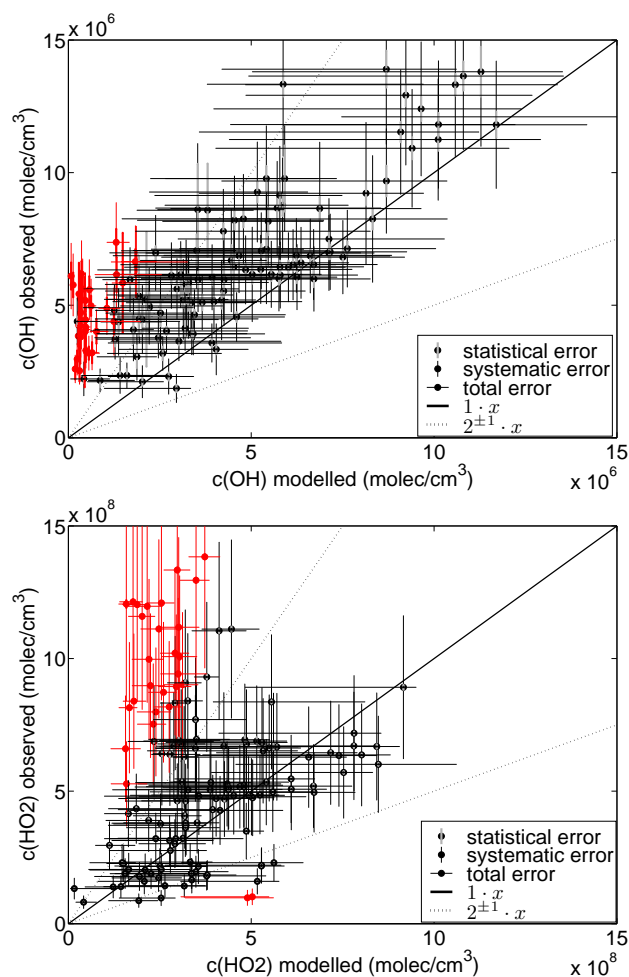ncertainty of 15%. An uncertainty of $\approx$15% for the OH concentrations and $\approx$10% for the HO$_2$ concentrations were obtained. The largest impact on the OH concentrations, depending on the different measurement situations, had the following reactions: H$_2$O + O(^{1}D) $\rightarrow$ 2OH($\approx$9%), N$_2$ + O(^{1}D) $\rightarrow$ O(^{3}P) + N$_2$ ($\approx$6%), and ISOP + OH $\rightarrow$ ISO$_2$($\approx$10%). Their uncertainties are given to be < 20% (Sander et al., 2003). For the HO$_2$ radical the reaction of HO$_2$ + HO$_2$ $\rightarrow$ H$_2$O$_2$ and ISO$_2$ + HO$_2$ $\rightarrow$ ISOOH influenced the simulated HO$_2$ concentration of about 6% and 8%, respectively.

4   Results and discussion

To examine the radical chemistry over the tropical rainforest, diverse tropospheric conditions (e.g. time of day, altitude, background air) were covered by the flight tracks performed

Table 4. Sensitivity studies with MECCA concerning the constrained measured species. Concentrations are mean values for the forest boundary layer (< 1 km) in the afternoon (14–17 LT).

	OH (molec/cm^3)	1σ (%)	OH obs/mod	HO$_2$ (molec/cm^3)	1σ (%)	HO$_2$ obs/mod
Observation	43.9×10^5	21	1.0	10.2×10^8	19	1.0
Reference Run	3.84×10^5	32	12.2±3.5	2.63×10^8	24	4.1±1.4
0.5 Isoprene	5.75×10^5	31	8.1±2.2	2.78×10^8	24	3.9±1.3
0.5 (MACR + MVK)	3.98×10^5	31	11.8±3.4	2.64×10^8	23	4.1±1.4
2 O$_3$	6.24×10^5	33	7.5±2.1	2.79×10^8	24	3.9±1.4
2 NO	4.42×10^5	32	10.7±3.4	2.90×10^8	23	3.7±1.3
2 H$_2$O	5.55×10^5	33	8.4±2.3	2.53×10^8	24	4.3±1.5
0.5 CO	3.84×10^5	33	12.2±3.5	2.58×10^8	24	4.2±1.4
3 H$_2$O$_2$	4.60×10^5	37	10.5±3.2	2.73×10^8	25	4.0±1.4
2 HCHO	3.96×10^5	30	11.8±3.5	3.57×10^8	25	3.1±1.1
0 Alkanes	3.92×10^5	32	11.9±3.4	2.63×10^8	23	4.1±1.4
0.3 ROOH	3.74×10^5	32	12.6±3.6	2.60×10^8	23	4.2±1.4
2 J(O^{1}D)	6.24×10^5	33	7.5±2.1	2.76×10^8	25	4.0±1.5

during GABRIEL. Air influenced by rainforest emissions as well as unaffected air over the ocean was sampled. Figure 8 shows the observed to modelled ratio for OH and HO$_2$ as a function of location. Over the ocean and at higher altitudes the agreement is fairly good for OH and HO$_2$ with a possible slight model underestimation of OH and an overestimation of HO$_2$. However over the rainforest at low altitudes, where the emission of hydrocarbons influences the chemistry, the divergence between model and observation increases strongly. These discrepancies are greater for the hydroxyl radical (up to factors of 15) than for HO$_2$ (up to factors of 5). The substantial underestimation of the simulation is an indication of the inadequacy of the hydrocarbon chemistry scheme adopted in the model.

The uncertainty estimation for observations and simulations are included in the analyses to define the significance of the discrepancies. Figure 9 shows the 1σ range of the observed and modelled data, derived from the measurement uncertainties of the species that constrain the model. Upper and lower estimates are obtained by varying all concentrations within the uncertainties to achieve maximum and minimum production of OH and HO$_2$, and conversion of HO$_2$ to OH. Although OH and HO$_2$ concentrations were often reproduced by the model within a factor 2, there was significant disagreement for several data points for which the simulated values were lower than the observations.

Further sensitivity studies of the model have been performed including the constraining parameters to identify the observed trace gases with the strongest influence on the HO$_x$ concentrations by varying the concentrations of the single observed species separately by factors ranging from 0 to 3. Their influence on the HO$_x$ concentration is shown for

afternoon data over the rainforest in Table 4. The strongest sensitivities with respect to OH result from ozone photo dissociation and subsequent reaction with water vapour (163% and 145%, respectively), responsible for the primary production, and from isoprene (150%). The simulations of HO$_2$ are less sensitive to the applied variations, with the largest influence from formaldehyde (136%). Thus, the variation of any single constrained parameter by a factor of 2 is not sufficient to eliminate the discrepancy between the simulated and observed OH and HO$_2$ concentrations.

The role of formaldehyde was also investigated by simulating the HO$_x$ concentration simultaneously with HCHO. The unconstrained HCHO-simulations led to 1% more OH and 4% more HO$_2$ in average for the boundary layer over the rainforest in the afternoon, compared to the basic run. Therefore no significant effect in relation with the HCHO concentrations could be distinguished.

Additional uncertainties in the OH and HO$_2$ measurements due to possible interferences inside the instrument had been investigated during the intercomparison campaign HO$_x$ COMP in summer 2005. Under various tropospheric conditions, all instruments, including different measurement techniques, showed high linear correlation coefficients for daytime OH and HO$_2$ concentrations (Schlosser et al., 2009; Fuchs et al., 2010). For photolysis frequencies J(O^{1}D) $> 5 \times 10^{-8}$ s^{-1} no interference due to O$_3$, NO$_x$, RO$_x$, VOCs could be detected for the OH and HO$_2$ measurements. Small dependencies on the H$_2$O concentration were found for the HO$_2$ observations, being only relevant for small water mixing ratios (< 0.6%). The high correlation with the absolute measurement technique DOAS gives confidence in the performance of our LIF instrument, especially for the conditions during
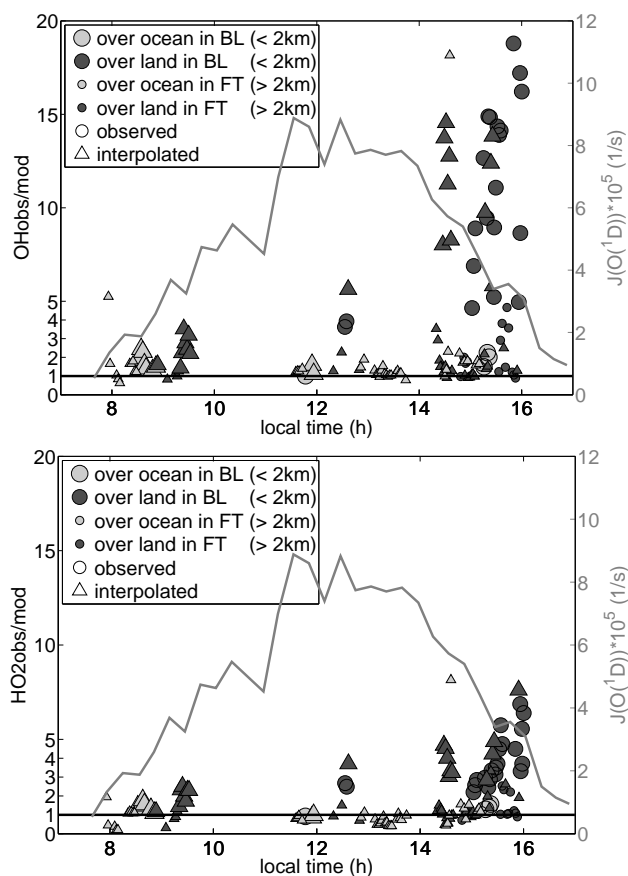
Fig. 10. Comparison of measurements and model results as a function of time, divided into two altitude regions: boundary layer (BL) <2 km and free troposphere (FT) >2 km.

Fig. 11. Observed isoprene mixing ratios with their measurement uncertainties for altitudes <1 km over the rainforest.
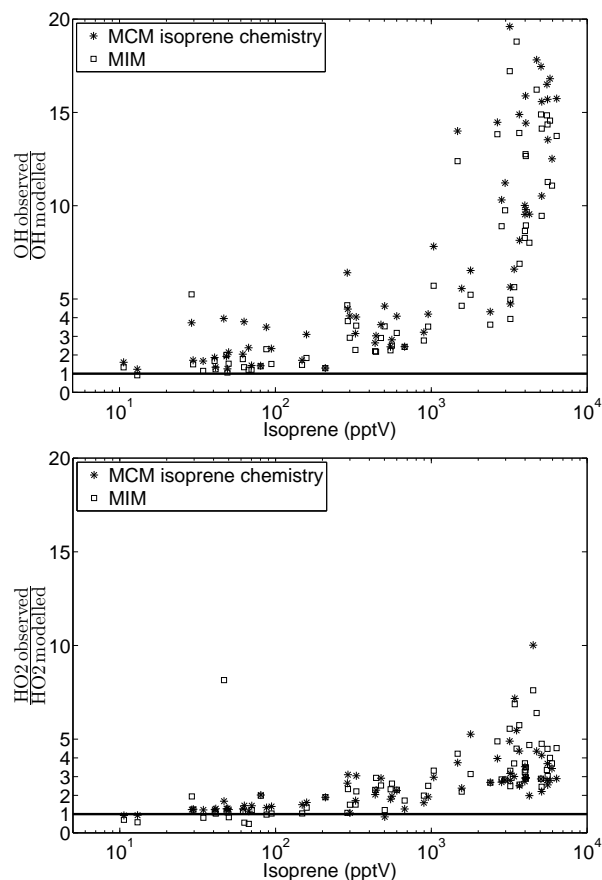
Fig. 12. Deviations between observations and model results as a function of isoprene mixing ratios.

the GABRIEL campaign. The performance of the LIF instrument for the detection of OH and HO$_2$ is also discussed in Martinez et al. (2010).

The rate constants of the used chemical mechanism of MECCA correspond to former recommendations and the rate constants should be updated in further studies. The recommended rate coefficients of Sander et al. (2006) for O(^{1}D)+H$_2$O, O(^{1}D)+O$_2$, O(^{1}D)+N$_2$, compared to Sander et al. (2003) account for a 12% reduction of OH and a 5% reduction for HO$_2$. For our studies, this effect lies within our uncertainty and does not change our conclusions. Therefore, to be consistent with Stickler et al. (2007), who analysed the GABRIEL data with a different focus on HCHO, MECCA v0.1p was used.

4.1 Correlation with isoprene

Comparison between observations and model simulations for OH and HO$_2$ with respect to the diurnal cycle, shows that model underestimations are relatively large in the afternoon, especially in the boundary layer (Fig. 10). Emissions of
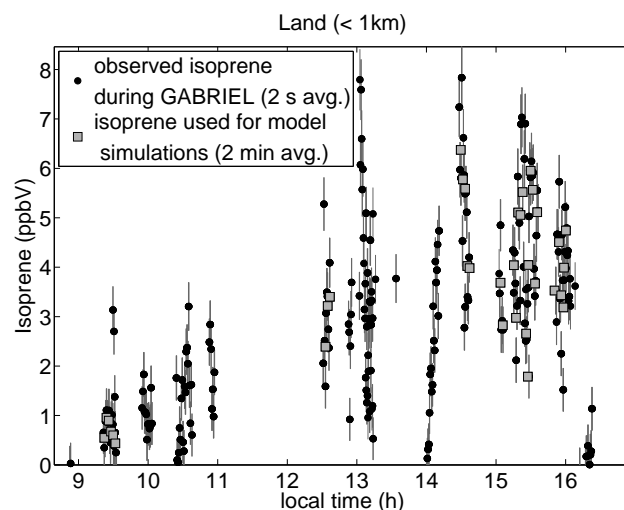
Table 5. Isoprene mechanism in MECCA. The entire chemical mechanism is described in the accompanying Supplement.

$ISOP + O_3$	$\longrightarrow$	$0.28HCOOH + 0.65MVK + 0.1MVKO_2 + 0.1PA + 0.14CO + 0.58HCHO + 0.09H_2O_2 +$	
		$+0.08CH_3O_2 + 0.25OH + 0.25HO_2,$	$k = 7.86 \times 10^{-15} e^{\frac{-1913}{T}}$
$ISOP + OH$	$\longrightarrow$	$ISO_2,$	$k = 2.54 \times 10^{-11} e^{\frac{410}{T}}$
$ISOP + NO_3$	$\longrightarrow$	$ISON,$	$k = 3.03 \times 10^{-12} e^{\frac{-446}{T}}$
$ISO_2 + HO_2$	$\longrightarrow$	$ISOOH,$	$k = 2.22 \times 10^{-13} e^{\frac{1300}{T}}$
$ISO_2 + NO$	$\longrightarrow$	$0.956NO_2 + 0.956MVK + 0.956HCHO + 0.956HO_2 + 0.044ISON,$	
			$k = 2.54 \times 10^{-12} e^{\frac{360}{T}}$
$ISO_2 + CH_3O_2$	$\longrightarrow$	$0.5MVK + 1.25HCHO + HO_2 + 0.25MGLO + 0.25ACETOL +$	
		$+0.25CH_3OH,$	$k = 2.0 \times 10^{-12}$
$ISO_2 + ISO_2$	$\longrightarrow$	$2MVK + HCHO + HO_2,$	$k = 2.0 \times 10^{-12}$
$ISOOH + OH$	$\longrightarrow$	$MVK + OH,$	$k = 1.0 \times 10^{-10}$
$ISON + OH$	$\longrightarrow$	$ACETOL + NACA,$	$k = 1.3 \times 10^{-11}$
$ISOOH + h\nu$	$\longrightarrow$	$MVK + HCHO + HO_2 + OH$	$J = J_{CH_3OOH}$
$ISON + h\nu$	$\longrightarrow$	$MVK + HCHO + NO_2 + HO_2$	$J = 3.7 J_{PAN}$
$MVK + O_3$	$\longrightarrow$	$0.45HCOOH + 0.9MGLO + 0.1PA + 0.19OH + 0.22CO + 0.32HO_2,$	
			$k = 0.5(1.36 \times 10^{-15} e^{\frac{-2112}{T}} + 7.51 \times 10^{-16} e^{-\frac{1521}{T}})$
$MVK + OH$	$\longrightarrow$	$MVKO_2,$	$k = 0.5(4.1 \times 10^{-12} e^{\frac{452}{T}} + 1.9 \times 10^{-11} e^{\frac{175}{T}})$
$MVKO_2 + HO_2$	$\longrightarrow$	$MVKOOH,$	$k = 1.82 \times 10^{-13} e^{\frac{1300}{T}}$
$MVKO_2 + NO$	$\longrightarrow$	$NO_2 + 0.25PA + 0.25ACETOL + 0.75HCHO + 0.25CO + 0.75HO_2 + 0.5MGLO$	
			$k = 2.54 \times 10^{-12} e^{\frac{360}{T}}$
$MVKO_2 + NO_2$	$\longrightarrow$	$MPAN,$	$k = 0.25k_{3rd}(T, M, 9.7 \times 10^{-29}, 5.6, 9.3 \times 10^{-12}, 1.5, 0.6)$
$MVKO_2 + CH_3O_2$	$\longrightarrow$	$0.5MGLO + 0.375ACETOL + 0.125PA + 1.125HCHO + 0.875HO_2 + 0.125CO +$	
		$+0.25CH_3OH,$	$k = 2.0 \times 10^{-12}$
$MVKO_2 + MVKO_2$	$\longrightarrow$	$ACETOL + MGLO + 0.5CO + 0.5HCHO +$	
		$+HO_2,$	$k = 2.0 \times 10^{-12}$
$MVKOOH + OH$	$\longrightarrow$	$MVKO_2,$	$k = 3.0 \times 10^{-12}$
$MVK + h\nu$	$\longrightarrow$	$PA + HCHO + CO + HO_2$	$J = 0.019 J_{COH_2} + 0.015 J_{CH_3COCHO}$
$MVKOOH + h\nu$	$\longrightarrow$	$OH + 0.5MGLO + 0.25ACETOL + 0.75HCHO + 0.75HO_2 + 0.25PA + 0.25CO$	
			$J = J_{CH_3OOH}$

ISOP = isoprene, ISO_2 = isoprene (hydroxy) peroxy radicals, ISOOH = isoprene (hydro) peroxides, ISON = organic nitrates from ISO_2 and $ISOP+NO_3$, MVK = methylvinylketone + methacrolein, $MVKO_2$ = MVK/MACR peroxy radicals, MVKOOH = MVK/MACR hydroperoxides, MGLO = methylglyoxal, PA = peroxy acetyl radical, NACA = nitro-oxy acetaldehyde, MPAN = peroxymethacryloyl nitrate + peroxymethacrylic nitric anhydride, ACETOL = hydroxy acetone. Reactions are taken from the MECCA v0.1p.

$$k_{3rd}\left(T, [M], k_0^{300}, n, k_\infty^{300}, m, f_c\right) = k_0(T)[M]\left(1 + \frac{k_0(T)[M]}{k_\infty(T)}\right)^{-1} f_c^{\left\{1 + \lg^2\left(\frac{k_0(T)[M]}{k_\infty(T)}\right)\right\}^{-1}}, \quad k_0(T) = k_0^{300}(\frac{300}{T})^n, k_\infty(T) = k_\infty^{300}(\frac{300}{T})^m.$$

hydrocarbons from the rainforest are driven by light and temperature. The most abundant VOC species over the rainforest is isoprene (Guenther et al., 1995; Granier et al., 2000), the concentration of which increases strongly towards the afternoon (Fig. 11) (Eerdekens et al., 2008; Warneke et al., 2001). The initial reactions of the isoprene oxidation scheme in MECCA are given in Table 5.

The ratio of observation to model results for both OH and HO_2 as a function of the mixing ratio of isoprene is indeed clearly correlated, as shown in Fig. 12. For isoprene mixing ratios below 200 pptV, the ratios of observation to model concentrations vary around 1.4 ± 0.4 for OH and 1.0 ± 0.4 for HO_2, whereas for mixing ratios greater than 200 pptV the model increasingly underestimates the HO_x concentrations

by more than a factor of 2. Dividing into isoprene logarithmic bins of $\Delta \ln x = 0.5$, x: isoprene mixing ratio, leads to maximum observed to modelled ratios of 13 ± 2 (OH) and 3.7 ± 0.8 (HO_2) for the highest isoprene mixing ratios of 5.6 ± 0.4 ppbV. A similar observation was made by Ren et al. (2008), who measured HO_x over a forest in the northern mid-latitudes. Their photochemical box model (Crawford et al., 1999) overestimated OH for isoprene mixing ratios lower than 500 pptV, and increasingly underestimated the concentrations for isoprene levels exceeding 500 pptV. Although the absolute values differ from the GABRIEL studies, the performance of both models shows a similar tendency with respect to isoprene. The coincidence of the qualitative behaviour of the two

Table 6. Sensitivity studies of the photolysis frequencies concerning the isoprene chemistry of the MCM. Concentrations are mean values for the forest boundary layer (< 1 km) in the afternoon (14–17 LT).

	OH (molec/cm^3)	1σ (%)	OH obs/mod	HO$_2$ (molec/cm^3)	1σ (%)	HO$_2$ obs/mod
Observation	43.9×10^5	21	1.0	10.2×10^8	19	1.0
Reference Run	3.71×10^5	26	13.2 ± 3.9	3.00×10^8	23	3.8 ± 1.3
$10^3 \times$ J(MACR$_{18}$)[a]	2.48×10^5	39	21.5 ± 10.4	32.2×10^8	21	0.4 ± 0.1
$10^{-3} \times$ J(MACR$_{18}$)	3.67×10^5	27	13.3 ± 3.9	2.84×10^8	24	4.0 ± 1.4
$10^3 \times$ J(MACR$_{19}$)[b]	0.17×10^5	47	338 ± 183	29.6×10^8	21	0.4 ± 0.1
$10^{-3} \times$ J(MACR$_{19}$)	3.71×10^5	26	13.2 ± 3.8	2.79×10^8	24	3.9 ± 1.4
$10^3 \times$ J(MVK$_{24}$)[c]	4.48×10^5	26	11.0 ± 3.7	8.79×10^8	22	1.3 ± 0.5
$10^{-3} \times$ J(MVK$_{24}$)	3.71×10^5	26	13.2 ± 3.9	2.99×10^8	23	3.8 ± 1.3
$10^3 \times$ J(ISOPBOOH)[d]	4.62×10^5	26	10.5 ± 2.9	3.73×10^8	21	3.0 ± 1.0
$10^{-3} \times$ J(ISOPBOOH)	3.68×10^5	26	13.3 ± 4.0	2.97×10^8	24	3.8 ± 1.3
$10^3 \times$ J(ISOPDOOH)[e]	4.16×10^5	26	11.7 ± 3.4	3.27×10^8	23	3.5 ± 1.2
$10^{-3} \times$ J(ISOPDOOH)	3.70×10^5	26	13.2 ± 3.9	2.99×10^8	23	3.8 ± 1.3
$10^3 \times$ J(CH$_3$OOH$_{41}$)[f]	4.06×10^5	25	12.0 ± 3.4	3.29×10^8	22	3.4 ± 1.1
$10^{-3} \times$ J(CH$_3$OOH$_{41}$)	3.70×10^5	26	13.2 ± 3.9	2.98×10^8	24	3.8 ± 1.3

[a] MACR + h$\nu \longrightarrow$ CH$_3$CO$_3$ + HCHO + CO + HO$_2$

[b] MACR + h$\nu \longrightarrow$ MACO$_3$ + HO$_2$

[c] MVK + h$\nu \longrightarrow$ CH$_3$CO$_3$ + HCHO + CO + HO$_2$

[d] ISOPBOOH + h$\nu \longrightarrow$ ISOPBO + OH; J(ISOPBOOH) = J(CH$_3$OOH$_{41}$)

[e] ISOPDOOH + h$\nu \longrightarrow$ ISOPDO + OH; J(ISOPDOOH) = J(CH$_3$OOH$_{41}$)

[f] CH$_3$OOH + h$\nu \longrightarrow$ CH$_3$O + OH

different box models for different field campaigns points either to a more fundamental gap in our knowledge of the isoprene degradation mechanism or to missing sources of OH with the same emission behaviour as isoprene.

4.2 Simulation with the Master Chemical Mechanism MCM

To test the performance of the lumped mechanism MIM, the more detailed isoprene chemistry of the MCM (Pinho et al., 2005) was included in the box model MECCA for comparison. More species (213 in total) were taken into account and the reaction scheme included several additional photolytic reactions. As the absorption cross sections and the quantum yields were not available for all implemented species, the photolysis frequencies (J) could not be calculated with the TUV model. Therefore, photolysis frequencies for species for which this information was available were used for all species of similar chemical structure as grouped in the MCM. The resulting photolysis frequencies are very uncertain, therefore sensitivity studies concerning the photolytic reactions were performed by varying the J-values by a factor of 10^{-3} and 10^3. In order to avoid possible overestimation of H$_2$O$_2$, only the datasets with measured peroxide data available were taken into account. In Table 6, the photolytic reactions with the strongest effect on OH (more than 10% compared

to the base run) are listed. The photolysis frequencies of the two isomers of the isoprene peroxy radical (2-hydroperoxy-2-methylbut-3-en-1-ol (ISOPBOOH) and 2-hydroperoxy-3-methylbut-3-en-1-ol (ISOPDOOH)) were the most prominent. As recommended in the MCM, the photolysis frequency of CH$_3$OOH was used for the analysis, calculated with the absorption cross section given by Vaghjiani et al. (1989) with quantum yields of unity. Increasing this photolysis frequency by a factor of 10^3 enhanced OH and HO$_2$ concentrations by 24%. Reduction of any of these frequencies by a factor of 10^{-3} led to a maximum reduction of 2% in OH. Thus, photolysis reactions in the model with unknown photolysis frequencies, with respect to OH and HO$_2$, were not relevant unless the photolysis frequencies were very strongly underestimated.

Variation of the photolysis of methacrolein (MACR) has a strong impact on OH. However, the absorption cross sections for methylvinylketone (MVK) and MACR have been measured (Gierczak et al., 1997). The variation of a factor 10^3 was unrealistically high but emphasizes the effect of the photolysis products. Increasing the photolysis frequency of MACR by 10^3 led to a large underestimation of OH (Table 6), indicating that the products deplete OH in further reactions.

During GABRIEL only the total sum of MVK and MACR was measured. For the studies with the MCM mechanism, these two species are treated separately. A ratio of MVK :
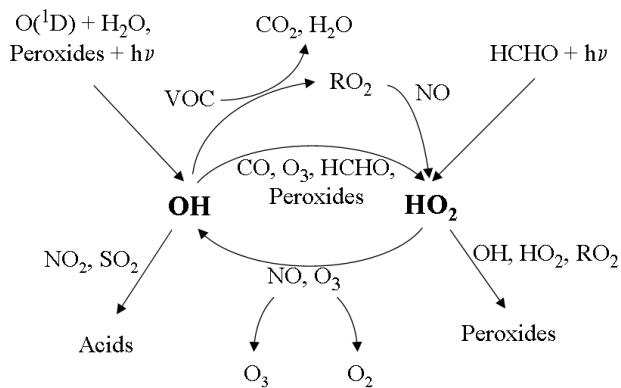
Fig. 13. Schematic representation of HO$_x$ cycling.

MACR $= 2:1$ was used (Kuhn et al., 2007). Simulations with ratios of MVK : MACR $= 0:1$ and $1:0$ changed the OH concentration about -5% and $+3\%$, the HO$_2$ concentration $+20\%$ and -10%, respectively. In MIM the two species are lumped together.

Although 493 more explicit reactions were considered in the extensive isoprene chemistry scheme of the MCM, similar results were obtained as for the lumped mechanism MIM (Fig. 12). The reduced chemical mechanism of MIM was developed on the basis of the MCM (Poeschl et al., 2000) and the results in Fig. 12 confirm that the MIM performs well within the original objective. Neither the simplification of the MIM chemistry nor the assumptions made for the MCM simulations explained the discrepancies between models and observations. Possible explanations might lead to more fundamental chemistry (Taraborrelli et al., 2009) or e.g. to segregation effects (Butler et al., 2008).

4.3 Testing the HO$_x$ cycling mechanism in MECCA

The HO$_x$ cycling mechanisms are illustrated in Fig. 13. In the remote troposphere OH is converted to HO$_2$ mainly via carbon monoxide and recycled from HO$_2$ by reactions with nitric oxide and ozone. However over the rainforest, OH is removed by reactions with the emitted VOC, producing peroxy radicals. These peroxy radicals react either with other peroxy radicals or NO forming HO$_2$, or with HO$_2$ producing peroxides. Total radical loss from the radical cycle occurs by removing OH, RO$_2$ and HO$_2$ from the system. One major loss pathway over the rainforest is the formation of organic peroxides. Although the photolysis of peroxides is also a source of radicals, this channel is minor compared to the radical production via photolysis of ozone and reaction with water vapour, or the photolysis of HCHO. Organic peroxides are also removed from the system by dry deposition (Stickler et al., 2007).

One possible reason for the underestimation of OH and HO$_2$ in the model is an overestimation of modelled radical removal through the production of organic peroxides,

especially the peroxides of isoprene and MACR+MVK (ISOOH, MVKOOH). Thornton et al. (2002) could explain their results from the SOS 1999 campaign (Nashville) for low NO$_x$ conditions by a decrease in the effective peroxide formation rate (RO$_2$ + HO$_2$ $\longrightarrow$ ROOH), which either means a reduction of the rate coefficient or a partitioning in an additional reaction e.g. RO$_2$ + HO$_2$ $\longrightarrow$ RO + OH + O$_2$. The latter has a functional equivalent to assumed rapid photolysis of ROOH. They found the best agreement for a decreasing factor of 10 in their box model. For the GABRIEL campaign about 50% of all RO$_2$ form ROOH, the other 50% forming HO$_2$ (branching ratio: $(RO_2 \rightarrow ROOH)/(RO_2 \rightarrow HO_2 + HCHO) = 1.0 \pm 0.2$) for isoprene mixing ratios > 2 ppbV, which are typical for the afternoon over the rainforest at altitudes below 1 km. Since photolysis of organic peroxides is negligible for radical production, as it is described by the chemical mechanism of MECCA, the sensitivity of HO$_x$ to the reaction rate of HO$_2$ with RO$_2$ can be investigated by taking these reactions out of the model.

For the HO$_2$ concentration this modified simulation leads to an enhancement factor of 2.5 ± 0.2 at maximum isoprene mixing ratios of (5.6 ± 0.4) ppbV, improving the comparison with the observation. However the influence on OH is small, leading to an increase only by a factor of 1.2 ± 0.1.

By constraining the HO$_2$ concentration to the observations, OH increases only by a factor of 1.7 ± 0.2. Thus the enhancement of HO$_2$ in the model does not imply an increase of OH sufficient to describe the observations, which instead requires additional recycling from HO$_2$ to OH in the model or additional direct sources for OH, as also proposed by Tan et al. (2001).

An additional OH recycling reaction, HO$_2$ + X $\longrightarrow$ OH + X$'$, is a possible pathway to increase the simulated OH concentration. As proposed by Thornton et al. (2002) and confirmed by the laboratory work of Hasson et al. (2004), certain alkyl peroxy radicals react with HO$_2$ yielding OH:

$$RO_2 + HO_2 \longrightarrow ROOH + O_2, \tag{R6}$$
$$\longrightarrow ROH \ + O_3, \tag{R7}$$
$$\longrightarrow RO + OH + O_2. \tag{R8}$$
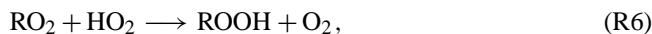
Such reactions would also decrease the organic peroxides which were overestimated by MECCA for GABRIEL (Stickler et al., 2007). Hasson et al. (2004) examined the additional Reaction (R8) for ethyl peroxy (C$_2$H$_5$O$_2$), acetyl peroxy (CH$_3$C(O)O$_2$) and acetonyl peroxy (CH$_3$C(O)CH$_2$O$_2$) radicals, finding a yield of 40% for acetyl peroxy radicals. Further studies concerning this type of reaction by Dillon et al. (2008) and Jenkin et al. (2007) showed similar results and typical yields of about 50% or higher. To assess the effect of this additional OH recycling, all RO$_2$ reactions with HO$_2$ were modified in MECCA without distinction between different species. The

branching ratio was varied between 50% and 90%, the latter obviously an upper limit. Nevertheless, even for the largest branching ratio the observed OH concentrations are still not reproduced. For the highest observed isoprene mixing ratios of (5.6 ± 0.4) ppbV the modification of MECCA produces maximum factors of 1.42 ± 0.04 and 2.42 ± 0.24 more OH for yields of 50% and 90% compared to the base runs (Fig. 14). This effect is still too small compared to the factors up to 13 needed to reproduce the measured OH concentrations under conditions of high isoprene. For HO$_2$ similar enhancement factors are obtained with 1.35 ± 0.06 and 1.99 ± 0.21 for the two OH yields, while factors of 3.7 are needed to reproduce the observations.

Another possible source of OH is the photolysis of organic peroxy radicals by near-infrared radiation via intramolecular rearrangement producing OH or HO$_2$ (Frost et al., 1999):

$$RO_2 + h\nu \longrightarrow R'O + OH, \qquad (R9)$$
$$\longrightarrow R'' + HO_2. \qquad (R10)$$

The photolysis frequency was assumed to follow that of NO$_3$ with values of 10^{-3} to $10^{-1} \times$ J(NO$_3$). The additional photochemical reactions were implemented in the model for all RO$_2$ to produce 100% OH via Reaction (R9), while no reaction channel to produce HO$_2$ was included. The highest photolysis frequency was chosen for the simulation shown here to obtain an upper limit (Fig. 14). For isoprene mixing ratios of (5.6 ± 0.4) ppbV the model with the additional chemistry leads to enhancement factors of 2.65 ± 0.56 for OH and 1.08 ± 0.02 for HO$_2$ compared to the base run. This is again insufficient to reproduce the observed HO$_x$ concentrations, even though the results represent an upper limit.

None of the proposed reaction amendments alone is sufficient to reproduce the measured data in the model. As a further step, both OH recycling reaction of RO$_2$ with HO$_2$ and infrared photolysis of RO$_2$ were included in the model reaction scheme with maximum yields for OH (90% yield for Reaction (R8) and $10^{-1} \cdot$ J(NO$_3$) for Reaction (R9)). Even then, simulated HO$_x$ remains too low with enhancement factors of 5.1 ± 1.1 for OH and 2.1 ± 0.2 for HO$_2$.

Searching for alternative reactions which leads to OH production and at the same time to a reduction of peroxides is a promising way to explain the measurements over the tropical rainforest. By constraining the box model with the observed OH and HO$_2$-concentrations overestimation of HCHO and peroxides could be found (Stickler et al., 2007). In this case isoprene oxidation produces more peroxy radicals and therefore more peroxides are produced. Alternative isoprene mechanisms, which reduce RO$_2$ and ROOH formation and were tested above, going in the right direction, but on its own are still not powerful enough.
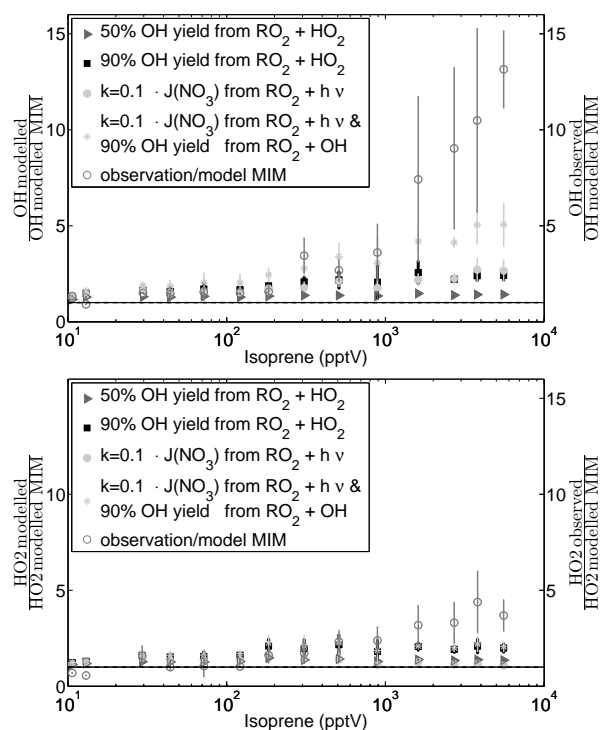

Fig. 14. Comparison of observed and modelled HO$_x$ based on selected changes in the MECCA chemistry scheme. Values are binned in isoprene mixing ratios (x) of $\Delta \ln x = 0.5$.

Ozonolysis of monoterpenes can also be an OH source (Tan et al., 2001) and is not considered in the model. As monoterpene emissions show a similar diurnal dependence as those of isoprene (Williams et al., 2007) their contribution to the OH concentration over the rainforest would be strongest in the afternoon. For the GABRIEL campaign α- and β-pinene were measured with maximum mixing ratios of the order of 200 pptV. Ozonolysis of monoterpenes was estimated to be about 10^5 molec cm^{-3} s^{-1} (Atkinson et al., 2005) over the rainforest in the afternoon, which is negligible compared to the primary production term (R1) of 3×10^6 molec cm^{-3} s^{-1}. The influence of monoterpenes and sesquiterpenes has been studied in detail by Ganzeveld et al. (2008), who compared the GABRIEL data with a single-column model, also concluding that ozonolysis of these species does not eliminate the large discrepancies between modelled and observed OH.

4.4 HO$_x$ budget

An overview of the most relevant reactions for the HO$_x$ budget in MECCA is given in Tables 7 and 8 to identify the main processes of the production and loss terms of OH and HO$_2$ for four groups of data. Case 1 is based on observations in the boundary layer over the rainforest, at altitudes lower than 1 km, in the morning (8–11 LT). Data from the same

Table 7. OH budget based on a model analysis of measurement data.

	case 1: land morning BL 6 data points	case 2: land afternoon BL 23 data points	case 3: ocean noon (3.5 ± 0.3) km 8 data points	case 4: land afternoon (3.3 ± 0.4) km 20 data points
production rate	$8.2 \times 10^6 \frac{\text{molec}}{\text{cm}^3\text{s}}$	$5.9 \times 10^6 \frac{\text{molec}}{\text{cm}^3\text{s}}$	$11.2 \times 10^6 \frac{\text{molec}}{\text{cm}^3\text{s}}$	$5.0 \times 10^6 \frac{\text{molec}}{\text{cm}^3\text{s}}$
$H_2O + O(^1D)$	36%	53%	61%	55%
$NO + HO_2$	46%	13%	9%	9%
$ISOOH + OH$	10%	15%	0%	9%
$H_2O_2 + h\nu$	4%	11%	19%	15%
$HO_2 + O_3$	2%	4%	6%	8%
$ISOOH + h\nu$	< 1%	2%	0%	< 1%
$ISOP + O_3$	< 1%	2%	0%	< 1%
remaining	2%	2%	5%	4%
loss rate	$-8.2 \times 10^6 \frac{\text{molec}}{\text{cm}^3\text{s}}$	$-5.9 \times 10^6 \frac{\text{molec}}{\text{cm}^3\text{s}}$	$-11.2 \times 10^6 \frac{\text{molec}}{\text{cm}^3\text{s}}$	$-5.0 \times 10^6 \frac{\text{molec}}{\text{cm}^3\text{s}}$
$Isop + OH$	39%	62%	0%	14%
$CO + OH$	13%	4%	35%	25%
$ISOOH + OH$	10%	15%	0%	9%
$CH_4 + OH$	6%	2%	12%	9%
$MVK + OH$	4%	6%	1%	5%
$MGLO + OH$	3%	3%	1%	3%
$HCHO + OH$	3%	2%	7%	3%
$MVKOOH + OH$	< 1%	< 1%	5%	6%
$CH_3OOH + OH$	< 1%	< 1%	10%	6%
$H_2O_2 + OH$	1%	< 1%	10%	5%
remaining	19%	6%	19%	15%
OH observed	$(5.3 \pm 1.6) \times 10^6 \frac{\text{molec}}{\text{cm}^3}$	$(4.4 \pm 0.9) \times 10^6 \frac{\text{molec}}{\text{cm}^3}$	$(12.5 \pm 1.1) \times 10^6 \frac{\text{molec}}{\text{cm}^3}$	$(5.2 \pm 1.6) \times 10^6 \frac{\text{molec}}{\text{cm}^3}$
OH modelled	$(2.1 \pm 0.8) \times 10^6 \frac{\text{molec}}{\text{cm}^3}$	$(0.4 \pm 0.1) \times 10^6 \frac{\text{molec}}{\text{cm}^3}$	$(10.1 \pm 0.7) \times 10^6 \frac{\text{molec}}{\text{cm}^3}$	$(3.2 \pm 2) \times 10^6 \frac{\text{molec}}{\text{cm}^3}$

location in the afternoon (14–17 LT) are analysed in the second group. Data from the free troposphere over the ocean at an altitude of 2–4 km around noon (11–14 LT) are used for case 3, and data collected over the rainforest in the afternoon at the same altitude for case 4. Only the cases with at least 6 data points are discussed. Data at altitudes higher than 4 km's are not considered, owing to the unavailability of measurements of peroxides, which become important for HO_x chemistry as H_2O concentrations decrease. The averaged concentrations of the species, which were used to constrain the simulations, are shown in Table 9.

The primary production of OH in the lower troposphere is the photolysis of ozone followed by reaction with water vapour. Primary production rates are of the order of 40%–60% of the total production. The NO mixing ratios are highest in the morning boundary layer over the forest with (65 ± 57) pptV, compared to (13 ± 9) pptV, (10 ± 3) pptV and (8 ± 4) pptV for the other three cases, respectively. In the morning, solar radiation is still low and the OH radical

recycling by reaction $NO + HO_2$ is comparable with the primary OH source. For all other cases the OH recycling via reaction of HO_2 is weak compared to the primary production. As the emissions of BVOCs increase during daytime, these compounds and their oxidation products increasingly influence the OH chemistry. The recycling of OH via the reactions of isoprene peroxides $ISOOH + OH$[2] in MIM is one of the major conversion mechanisms in MECCA and illustrates their importance to the chemistry of isoprene.

The loss of OH in the boundary layer, according to MECCA, is dominated by the reaction with isoprene. As isoprene concentrations increase during the day, the proportion of this reaction with respect to the total loss increases to 62% in the afternoon and is even more important than the primary production term (53%). When less isoprene is available, the removal of OH by CO and peroxides becomes more significant.
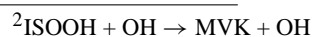
---

[2]$ISOOH + OH \rightarrow MVK + OH$

Table 8. HO$_2$ budget based on a model analysis of measurement data.

	case 1: land morning BL 6 data points	case 2: land afternoon BL 23 data points	case 3: ocean noon (3.5 ± 0.3) km 8 data points	case 4: land afternoon (3.3 ± 0.4) km 20 data points
production rate	$6.4 \times 10^6 \frac{\text{molec}}{\text{cm}^3\text{s}}$	$4.3 \times 10^6 \frac{\text{molec}}{\text{cm}^3\text{s}}$	$9.2 \times 10^6 \frac{\text{molec}}{\text{cm}^3\text{s}}$	$3.4 \times 10^6 \frac{\text{molec}}{\text{cm}^3\text{s}}$
HCHO + hν	13%	36%	15%	18%
CO + OH	17%	6%	42%	35%
ISO$_2$ + NO	32%	22%	0%	3%
ISO$_2$ + ISO$_2$	1%	8%	0%	< 1%
CH$_3$O$_2$ + NO	15%	5%	6%	8%
MVKO$_2$ + NO	3%	3%	< 1%	2%
HCHO + OH	4%	2%	8%	4%
ISOOH + hν	< 1%	3%	0%	< 1%
CH$_3$H$_6$O$_2$ + NO	4%	< 1%	0%	< 1%
H$_2$O$_2$ + OH	1%	< 1 %	12%	8%
remaining	14%	16%	16%	22%
loss rate	$-6.4 \times 10^6 \frac{\text{molec}}{\text{cm}^3\text{s}}$	$-4.3 \times 10^6 \frac{\text{molec}}{\text{cm}^3\text{s}}$	$-9.2 \times 10^6 \frac{\text{molec}}{\text{cm}^3\text{s}}$	$-3.4 \times 10^6 \frac{\text{molec}}{\text{cm}^3\text{s}}$
NO + HO$_2$	59%	17%	12%	13%
HO$_2$ + O$_3$	3%	5%	7%	11%
ISO$_2$ + HO$_2$	15%	44%	0%	15%
HO$_2$ + HO$_2$	17%	21%	48%	30%
CH$_3$O$_2$ + HO$_2$	2%	3%	16%	13%
MVKO$_2$ + HO$_2$	2%	6%	6%	11%
HO$_2$ + OH	1%	< 1%	9%	4%
remaining	1%	1%	2%	3%
HO$_2$ observed	$(6.3 \pm 0.5) \times 10^8 \frac{\text{molec}}{\text{cm}^3}$	$(10.2 \pm 1.9) \times 10^8 \frac{\text{molec}}{\text{cm}^3}$	$(5.7 \pm 0.6) \times 10^8 \frac{\text{molec}}{\text{cm}^3}$	$(4.7 \pm 1.5) \times 10^8 \frac{\text{molec}}{\text{cm}^3}$
HO$_2$ modelled	$(2.9 \pm 0.2) \times 10^8 \frac{\text{molec}}{\text{cm}^3}$	$(2.6 \pm 0.6) \times 10^8 \frac{\text{molec}}{\text{cm}^3}$	$(7.0 \pm 1.2) \times 10^8 \frac{\text{molec}}{\text{cm}^3}$	$(3.3 \pm 1.3) \times 10^8 \frac{\text{molec}}{\text{cm}^3}$

Table 9. Averaged mixing ratios for the parameters which constrain the box model simulations. The values are given for the four cases in Table 7 and 8 with their 1σ variability.

| Species	case 1	case 2	case 3	case 4
CO (ppbV)	94 ± 5	122 ± 13	100 ± 12	101 ± 7
Isoprene (ppbV)	0.7 ± 0.2	4.3 ± 1.2	0	0.2 ± 0.2
MVK+MACR (ppbV)	0.2 ± 0.1	1.6 ± 0.5	0.03 ± 0.02	0.2 ± 0.3
O$_3$ (ppbV)	14 ± 0.1	17 ± 4	29 ± 5	35 ± 9
NO (pptV)	65 ± 57	13 ± 9	10 ± 3	8 ± 4
H$_2$O (mmol/mol)	24 ± 0.5	23 ± 2	11 ± 1	9 ± 2
H$_2$O$_2$ (ppbV)	1.0 ± 0.1	2.2 ± 1.8	3.9 ± 1.2	2.3 ± 1.6
ROOH (ppbV)	0.5 ± 0.2	1.4 ± 0.6	1.0 ± 0.2	0.9 ± 0.5
HCHO (ppbV)	0.6 ± 0.3	1.2 ± 0.4	0.5 ± 0.4	0.4 ± 0.5
Acetone (ppbV)	0.6 ± 0.1	1.1 ± 0.2	0.7 ± 0.2	0.6 ± 0.1
Methanol (ppbV)	0.9 ± 0.2	3.2 ± 0.4	2.3 ± 1.1	2.5 ± 0.5
J(O(^{1}D)) (10^{-5} s^{-1})	2.9 ± 0.2	2.5 ± 1.0	9.2 ± 0.3	3.4 ± 1.1
J(NO$_2$) (10^{-4} s^{-1})	91 ± 4	82 ± 26	175 ± 1	111 ± 27
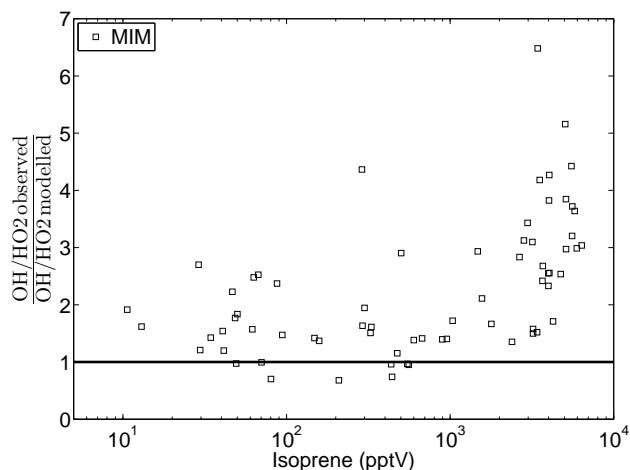
Fig. 15. Comparison of the ratio OH/HO_2 between observation and model as a function of isoprene.

The recycling reactions of RO_2+NO are the dominant processes for HO_2 production in the morning boundary layer over the forest (case 1), when NO concentrations are relatively high. When irradiation increases, photolysis of formaldehyde becomes an important source of the HO_2 radical (case 2). In the free troposphere the main source of HO_2 is the reaction of OH with carbon monoxide.

Recycling of OH by the reaction $NO+HO_2$ dominates the loss of HO_2 when morning NO is high within the forest boundary layer, initially not leading to radical loss. For the remaining cases the reaction with peroxy radicals and the self reaction, producing peroxides, are the major loss terms for HO_2. Since the photolysis of peroxides is slow to produce radicals, the production of peroxides effectively leads to removal of two radicals per reaction from the system.

Interconversion of HO_2 and OH via reactions with e.g. NO, O_3, CO and VOC (Fig. 13) can be characterized by the chain length of the reactions cycling between these two radicals. The HO_2/OH ratio in the forest boundary layer in the morning (case 1) shows a mean value of 127 ± 34 at mean NO mixing ratios of (65 ± 57) pptV. The value is comparable to results from Tan et al. (2001), who found HO_2/OH ratios of 80 - 120 for mean NO levels of 65.8 pptV over deciduous forest in northern latitudes. Simulation by MECCA slightly overestimates the ratio with $HO_2/OH =$ 156 ± 45. For the forest boundary layer in the afternoon (case 2) values of $HO_2/OH = 234 \pm 44$ were observed for mean NO mixing ratios of (13 ± 9) pptV . The model overestimates this ratio of HO_2 to OH by a factor of 3.2 ± 0.8, OH being underestimated more severely than HO_2 in the simulations. However, the correlation with the isoprene mixing ratio observed for OH and HO_2 (Fig. 12) is not significant for the ratio (Fig. 15) since the effect of isoprene on OH and HO_2 is similar for both radicals. The analysis of the different reactions relevant for the HO_x budget (Tables 7, 8) shows that

isoprene and its peroxy radicals are the major compounds responsible for HO_x loss ($\sim 50\%$) in the afternoon forest boundary layer. OH is directly removed by reaction with isoprene, producing the peroxy radical ISO_2, which either removes HO_2 from the system, forming the peroxide ISOOH (60%), or produces HO_2 and formaldehyde by reactions with RO_2 or NO (40%).

During the GABRIEL campaign Sinha et al. (2008) performed OH reactivity measurements within the canopy of the rainforest (about 35 m above the ground). 35% of their measured total OH reactivity is due to reaction of OH with isoprene, MVK+MACR, acetone, acetaldehyde and methane, whereas 65% could not be explained by the measured species. They proposed that the missing fraction of the total reactivity is possibly due to unmeasured reactive compounds. For our studies this would lead to even larger discrepancies between the observation and the box model simulations. However our aircraft measurements and the OH reactivity measurements of Sinha et al. (2008) were made at different altitudes. Highly reactive unmeasured compounds, emitted from the rainforest, might only play an significant role inside the canopy and might be too short-lived to reach the sampling area of the aircraft above 300 m.

4.5 Recycling probability and missing source strength for OH

To determine the recycling strength of the chemical system, the recycling probability has been calculated. The OH recycling probability r is defined as (Lelieveld et al., 2002):

$$r = \frac{S}{P+S}, \tag{1}$$

with P and S being the primary and secondary production, respectively. The primary production is considered to be only the reaction of $O(^1D) + H_2O$, whereas photolysis of peroxides and recycling reactions of HO_2 are assumed to be secondary productions terms, as the reactants are oxidation products in the OH oxidation chain. The base simulation of MECCA yields $P = 3.12 \times 10^6$ moleccm^{-3}s^{-1} and $S = 1.94 \times 10^6$ moleccm^{-3}s^{-1} and therefore $r =$ 0.38 for boundary layer values over the forest in the afternoon (case 2). The total loss term L in steady state simulations is equal to the total production term G with $L = G = P + S = 5.06 \times 10^6$ moleccm^{-3}s^{-1}. Calculations using measured higher OH and HO_2 to constrain the box model, containing the same chemical mechanism, leads to $P = 3.12 \times 10^6$ moleccm^{-3}s^{-1} and $S = 3.53 \times 10^6$ moleccm^{-3}s^{-1}. The total production term is therefore $G = 6.65 \times 10^6$ moleccm^{-3}s^{-1} compared to the total loss term of $L = 56.64 \times 10^6$ moleccm^{-3}s^{-1}, calculated with MECCA constrained by the HO_x observations. Thus, a production rate term of the order $S^* = 5 \times 10^7$ moleccm^{-3}s^{-1} is missing. Adding the missing term as secondary production would lead to a recycling probability
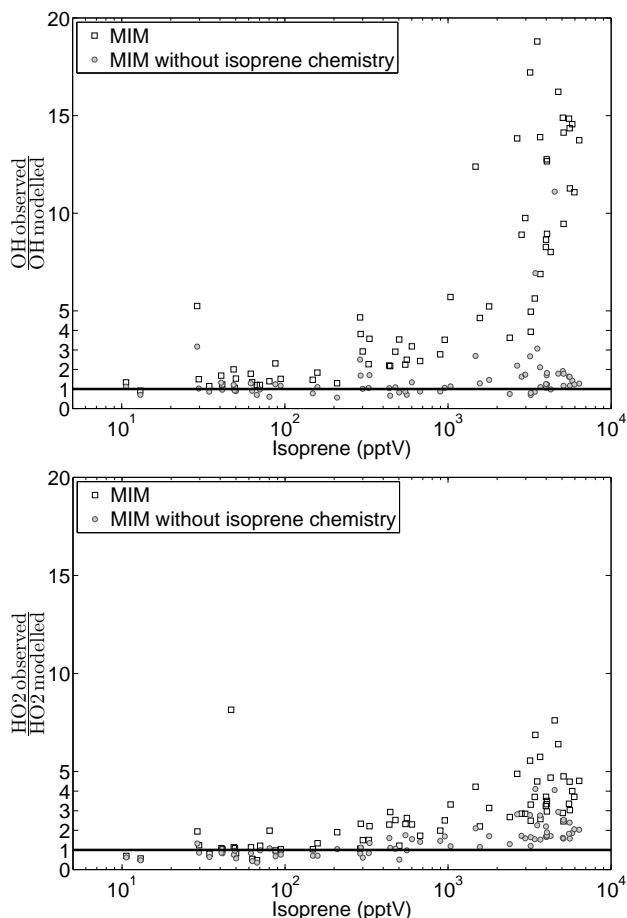
Fig. 16. Ratio of observed and modelled OH and HO$_2$ concentrations as a function of isoprene and other conditions observed simultaneously with isoprene.

Fig. 17. Comparison between observation and a model run including the additional HO$_x$ reaction: ISO$_2$ + HO$_2$ → ISOOH + nOH and ISOP + OH → ISO$_2$ + mOH. Values are binned in isoprene mixing ratios (x) of $\Delta \ln x = 0.5$.

due to the observation of $r = 0.94$. Considering that this value of r is very high, it may be speculated that part of the missing OH formation is related to primary formation involving O$_3$. Previously it has been indicated that reactions of O$_3$ with reactive terpenes might be important (Tan et al., 2001; Di Carlo et al., 2004; Goldstein et al., 2004). Alternatively, O$_3$ may react with reaction products in the isoprene degradation pathway, produce OH and reduce the discrepancy, which would moderate the OH recycling probability.

The missing term S^* is comparable to the loss rate of OH through direct reaction with isoprene. By neglecting the entire isoprene chemistry in the box model MECCA, good agreement between simulations and HO$_x$ observations is obtained, independent of the isoprene concentrations that were observed (Fig. 16). This indicates that the reason for the model underestimations rather lies in the oxidation mechanism of isoprene than in missing direct sources. An observed to modelled ratio of 1.3 ± 0.5 for OH is found
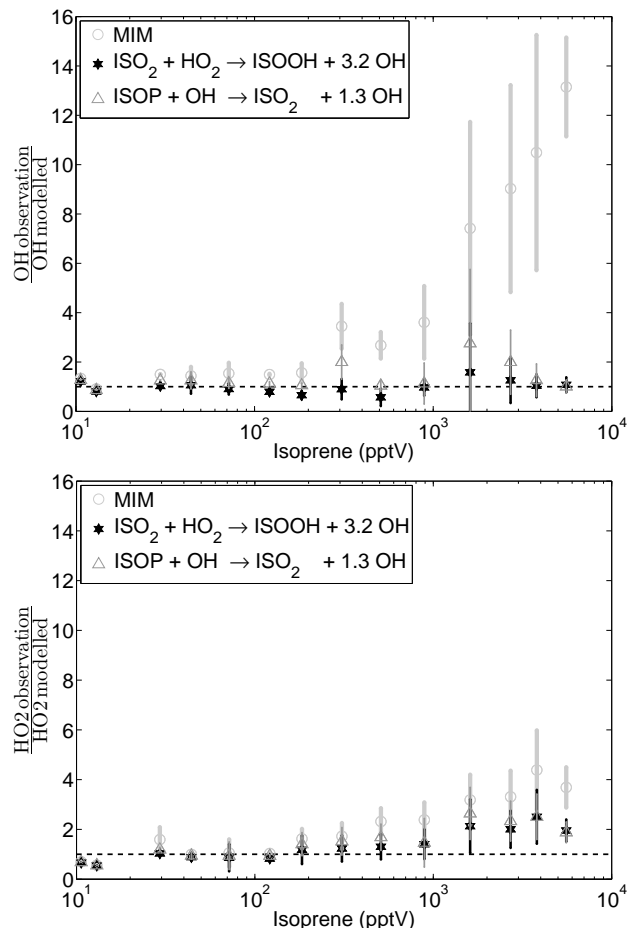
for all measured isoprene mixing ratios. The situation for HO$_2$ is somewhat different. For low isoprene (< 200 pptV) the model now tends to overestimate HO$_2$, but is still well described within the uncertainty (0.9 ± 0.3). In contrast to OH, the dependence on the isoprene concentration is still discernable, though small, possibly indicating an additional influence on HO$_2$ by other trace gases also dependent on the time of day.

Butler et al. (2008) analysed the GABRIEL dataset using a global model. Analogous to the implementations of Reaction (R8) in our model, they introduced a modification of the reaction of the isoprene peroxy radical ISO$_2$ with HO$_2$ producing $n \cdot$OH in their reaction scheme:

$$\text{ISO}_2 + \text{HO}_2 \longrightarrow \text{ISOOH} + n \text{ OH}. \qquad \text{(R11)}$$
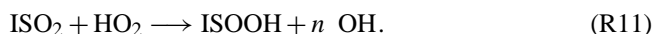
An optimum number of $n = 2$ was derived to best reproduce the OH observations. For our constrained box model the best agreement between observation and simulation was found for $n = 3.2$ (Fig. 17). A mean measured to modelled ratio of 1.0 ± 0.3 was obtained for OH and the dependence on isoprene disappeared.

Reaction (R11) should be understood as a proxy for additional recycling within the isoprene chemistry. The equivalent reaction:

$$ISOP + OH \longrightarrow ISO_2 + m \ OH. \tag{R12}$$

with best agreement for $m = 1.3$ shows that regarding the initial step in the oxidation mechanism more OH has to be produced than destroyed. A mean value for the observed to model ratio of 1.4 ± 0.5 was calculated (Fig. 17). Additional sources of OH, comparable and correlated to the isoprene sink are needed to describe the observations. Unknown OH recycling within the isoprene oxidation mechanism seems the most likely way to provide the additional OH source, leading to a much larger oxidation capacity of the atmosphere over the tropical rainforest.

5 Follow up studies to the GABRIEL campaign

During GABRIEL the first reported measured HO$_x$ concentrations over a tropical rainforest were found to be significantly higher than predicted by current models. Whereas studies performed in remote areas or distant from direct VOC emissions showed a rather good agreement (Whalley et al., 2010), studies close to biogenic VOC sources generally reported higher OH concentrations under low NO$_x$ conditions than expected.

Former measurements of HO$_x$ radicals over deciduous forests in the mid latitudes have shown significant underestimations of the observed OH concentration compared to box model simulations (Tan et al., 2001; Carslaw et al., 2001; Ren et al., 2008). Tan et al. (2001) found a deviation by a factor of ~ 3 for the OH radicals, particularly for low NO$_x$ and high isoprene conditions. Carslaw et al. (2001) also simulated 50% less OH than measured at averaged isoprene levels of 2 pbbv. Analyses of Ren et al. (2008) showed, consistent with this study, a correlation of the deviations between simulations and observations with the isoprene concentrations. Although the values of model to measured OH ratio vary for the different measurement conditions, all box models show an underestimation of the observed OH concentrations, indicating a general inconsistency of the radical chemistry in box models for biogenic low NO$_x$ regions.

It is well known that the tropical rainforest are a major source of BVOCS, which up to now were predicted to suppress the oxidation capacity of the atmosphere. However, the unexpected results of the GABRIEL campaign have reflected the lack of knowledge in describing the chemical

processes over these important regions and therefore have initiated worldwide research in this field. More HO$_x$ measurements in and over the tropical rainforest followed, like the OP3 and AMMA campaign in Borneo and West Africa, respectively (Hewitt et al., 2010; Commane et al., 2010). Both campaigns reported daily maximum OH concentrations up to 8.7×10^6 molec cm^{-3} and 0.6 pptV on ground, respectively. Although higher NO concentrations were observed, the OH concentrations are comparable to those of GABRIEL (~ 0.5 pptV i.e. 6×10^6 molec cm^{-3}, Martinez et al., 2010). Unfortunately due to technical problems, the observed OH-concentrations over West Africa were rarely above the detection limit, so that a model-to-measurement comparison was not possible (Stone et al., 2010). However for a point-to-point comparison model simulations by Saunois et al. (2009) might indicate an underestimation by a factor of 2, whereas Stone et al. (2010) conclude a possible overestimation of the model. The overestimation could be caused by the higher observed NO concentrations (~ 51 pptV, Stone et al., 2010), in contrast to the low NO regime of GABRIEL, where the largest deviations were found at NO ≈ 13 pptV. However comparison of the Borneo data with the box model (CiTTyCAT) again showed an underestimation of the observed concentration by a factor of ~ 3, being in a NO regime of about 37 pptV (Pugh et al., 2010a).

Measurements in the polluted Pearl River Delta, China, showed a good agreement with model calculations for high NO concentrations (>1 ppbv), whereas under high VOC and moderately low NO conditions (<200 pptV) measured OH is 3 to 5 times higher than expected by our current understanding (Hofzumahaus et al., 2009). However, compared to the low NO concentrations during GABRIEL, where the reaction between RO$_2$ + HO$_2$ are most dominant and might lead to unknown OH recycling, the situation in the Pearl River Delta is more determined by the competing reaction of RO$_2$ + NO. Therefore Hofzumahaus et al. (2009), similar to Tan et al. (2001), proposed another pathway of additional OH recycling via RO$_2$ + X $\longrightarrow$ HO$_2$ and HO$_2$ + X $\longrightarrow$ OH to gain sufficient OH production under moderately low NO conditions.

Containing the traditional chemistry different box models have been tested to find an explanation for the high HO$_x$ observations over the tropical rainforest. Taraborrelli et al. (2009) presented the improved version MIM2 of the MIM mechanism, derived as a reduction from the MCM scheme. The MIM2 model scheme has been applied for the GABRIEL conditions with low NO, as well as with medium and high NO concentrations. An increase of up to 15% in the calculated OH was feasible, but still the measurements of GABRIEL could not be explained. Archibald et al. (2009) applied eight different complex isoprene mechanisms by using high isoprene emissions rates (up to 6.4 mg m^{-2} h^{-1}, corresponding to about 1.6×10^{12} molec cm^{-2} s^{-1}), representative for tropical rainforest

conditions. Each model, independent from the complexity of the chemical mechanisms, simulated very low OH concentrations under low NO$_x$ conditions (OH daytime average of 10^5 molec cm^{-3}), confirming that all current isoprene mechanisms are unable to match the observed HO$_x$ concentrations. Model agreement could only be reached by including an additional OH source in the order of 2.0×10^7 molec cm^{-3} s^{-1}, dependent on the light controlled correction factor of the isoprene emissions, which is consistent with the GABRIEL results.

New possible reaction pathways for OH recycling within the isoprene oxidation mechanisms have further been investigated by quantum chemical calculations and have partly been tested by laboratory studies. A promising approach is the competing unimolecular reaction of certain RO$_2$ radicals via H-shift, which is predicted to lead to OH and/or HO$_2$ formation. For these reactions Peeters et al. (2009) calculated a yield of about 0.7 HO$_2$ and 0.03 OH radicals per isoprene oxidized, whereas Da Silva et al. (2010) suggest an yield up to 0.07 OH, both calculations done for pristine tropical rainforest conditions. Only theoretically proposed and not confirmed by laboratory measurements, this pathway alone is still not sufficient to describe the GABRIEL measurements. Nevertheless, possible photo labile coproducts, e.g. hydroperoxyaldehydes, with a unity yield become an additional OH source and might provide an explanation for the high observed OH concentration over the tropical rainforest. Another not yet fully incorporated mechanism for OH recycling is the formation of epoxides, which has been predicted by quantum chemical calculations and also found in chamber experiments (Paulot et al., 2009). Epoxides are of particular interest because of their potential to form SOA under low NO$_x$ conditions, which helps to resolve the open question of aerosol formation over the tropical rainforest (Kleindienst et al., 2009; Martin et al., 2010).

Implementation of the new proposed chemical mechanisms in box model simulations for tropical rainforest conditions was done by Archibald et al. (2010). Different scenarios were tested, showing the largest enhancement for modelled OH concentrations by including the discussed recycling reactions via RO$_2$ + HO$_2$, epoxide formation, unimolecular reactions of the RO$_2$ and photolysis of intermediates products. Applying the rate constants in their upper limits lead to 3.2 times more OH than the MCM scheme, which is consistent to the model results of this study. Within 30% the LIM0 (Leuven Isoprene Mechanism, Peeters et al., 2009) could explain the observed HO$_x$ concentrations during GABRIEL applied in global CTM calculations by Stavrakou et al. (2010). The scheme is characterised by fast elimination of O$_2$ from the hydroperoxy radicals, the 1,5- and 1,6-H-shift leading to OH and HO$_2$ formation, respectively, and a very fast photo dissociation of the hydroperoxy aldehydes producing additional OH and HO$_2$ radicals.

Beside the discussion of additional new chemical reactions and schemes to regenerate OH, the effect of simple segregation of air masses (Krol et al., 2000; Karl et al., 2007; Dlugi et al., 2010) and deposition of OH reactants (Pugh et al., 2010a) has been investigated. Segregation, originating from incomplete mixing between air enriched with VOC and air enriched with OH can lead to an apparent reduction of the reaction constants. Studies comparing box model with LES simulations by Krol et al. (2000) show an apparent reduction of the RH-OH reaction rate by 30%. Calculation of segregation over the Amazon rainforest during AMAZE-08, using water vapour as a proxy for unmeasured OH concentrations, showed a decrease of k(OH+ISOP) up to (39 ± 7)% in the 800-m-deep cloud layer (Karl et al., 2007), leading to higher simulated OH concentrations. Dlugi et al. (2010) calculated the intensity of segregation from highly time resolved trace gas measurements, including OH and isoprene, during the ECHO campaign in a deciduous forest in mid latitudes (Germany). For ECHO the authors demonstrated that the effective OH isoprene reaction rate is reduced by segregation by 15%. A similar segregation intensity of 15% was found during OP3 by Pugh et al. (2010b), using simulated OH concentrations from a box model and measured isoprene concentrations. All studies show that segregation contributes to an apparent reduction of the RH-OH reaction rate but cannot explain the magnitude of the discrepancy alone.

For ground based observations an increase of the deposition rates for OH reactants, like MACR and MVK, can help to to explain the measurement of the OP3 campaign in Borneo (Pugh et al., 2010a). By using a deposition rate of v_d(MACR + MVK) = 2.5 cm s^{-1} and reducing the reaction rate constant k (isoprene/monoterpenes + OH) by 50%, the OH-observations over the Borneo rainforest could be reproduced.

Currently several global models use a reduced isoprene emission rates of of 220–350 TgC yr^{-1} (Brasseur et al., 1998; Kuhlmann et al., 2003), which is much lower than observations have shown (500 TgC yr^{-1}, Guenther et al., 1995). The high OH concentrations, as observed during GABRIEL, reduce the lifetime of isoprene significantly, and might close the inconsistency in the isoprene flux.

The initial work done during GABRIEL, which is confirmed by measurements of other groups, indicate that in low NO environments the oxidation of biogenic VOC leads to more recycling and regeneration of OH then assumed until now.

6 Conclusions

Higher HO$_x$ concentrations over the tropical rainforest during the GABRIEL campaign were observed than predicted by the box model MECCA constrained by measurements. Observations and simulations agree fairly

well for the free troposphere, whereas maximum deviations were found for low altitudes (< 1 km) in the afternoon with mean discrepancy factors of 12.2 ± 3.5 and 4.1 ± 1.4 for OH and HO$_2$, respectively. These discrepancies are strongly correlated to isoprene emitted by the rainforest. However, the OH/HO$_2$ ratio does not show a significant dependence on isoprene, as OH and HO$_2$ are similarly influenced by isoprene. Simulations with the more detailed isoprene mechanism of the MCM leads to similar results as the MIM chemical reaction scheme, indicating that the original objective of using a condensed mechanism to reproduce the results of the MCM is still met.

In the simulations with MECCA radical loss from the system via removal of RO$_2$ producing organic peroxides, appears to be about 50% for air in the afternoon boundary layer. Sensitivity studies eliminating the production of organic peroxides increase the HO$_2$ and OH concentrations, but not sufficiently to achieve agreement with the observations.

Enhancement of photolysis frequencies of organic peroxides by unlikely factors of 10^3 do not provide a sufficient source for HO$_x$. Constraining the model to measured HO$_2$ enhances OH, but is also insufficient to match observations. Therefore, an additional production channel of OH is needed to explain the OH observed over the rainforest. Modification of the chemistry scheme of MECCA could not sufficiently enhance the the simulated HO$_x$ concentration, either by recycling of OH through reaction of peroxy radicals with HO$_2$ or through infrared photolysis of peroxy radicals, or by combining the two.

Constraining the HO$_x$ concentration in the simulations led to an overestimation of HCHO and peroxides, pointing to the importance of a large RO$_2$ production within the isoprene oxidation scheme (Stickler et al., 2007). Therefore alternative reaction pathways, producing OH and simultaneously reducing peroxide formation, is still a likely way, but must have a stronger effect (either combined or on their own) than the reactions tested in this study.

The major OH and HO$_2$ sources over the rainforest (<1 km) in the afternoon are the reaction of O(^{1}D) + H$_2$O and the photolysis of HCHO. When available in the atmosphere, isoprene and its oxidation products strongly influence the OH chemistry leading to a loss rate of OH in the model comparable to the primary production rate. A recycling probability of $r = 0.38$ follows from the standard simulation, whereas a value of up to $r = 0.94$ is needed to explain the observations. An OH source stronger than the loss rate owing to ISOP + OH is evidently missing in the chemical mechanism based on current understanding ($S^* = 5 \times 10^7$ molec cm^{-3} s^{-1}). By neglecting the isoprene chemistry in MECCA, the underestimation of the HO$_x$ simulations disappears. This leads to the hypothesis that the recycling of OH, mainly in the isoprene oxidation mechanism, is more efficient than predicted by the current reaction schemes. The additional

recycling reaction via ISOP + OH $\rightarrow$ ISO$_2$ + $m \cdot$ OH with $m = 1.3$ improves the agreement with the OH observations, and further investigations to unravel the detailed chemical mechanisms are recommended.

Following the GABRIEL campaign several approaches to understand the tropospheric chemistry over the tropical rainforest have been made by different research groups. Comparable OH concentrations were found over the tropical rainforest of West Africa and Borneo. Theoretical quantum chemical calculations as well as laboratory measurements have been performed to propose alternative reaction pathways inside the isoprene oxidation scheme. Box model simulations including these reactions often failed to explain the GABRIEL observations. Implying a high photo dissociation rate of the predicted intermediates the LIMO mechanism was able to reproduce the GABRIEL data within 30% in global CTM calculations (Stavrakou et al., 2010). Promising concepts have been proposed but still have to be confirmed by laboratory and field measurements. Explaining the high unexpected observed OH concentrations over the tropical rainforest remains a major task in atmospheric science.

Supplementary material related to this article is available online at:
http://www.atmos-chem-phys.net/10/9705/2010/
acp-10-9705-2010-supplement.pdf.

References

Archibald, A. T., Jenkin, M. E., Shallcross, D.E.: An isoprene mechanism intercomparison Atmos. Environ., in press, 1352–2310, doi:10.1016/j.atmosenv.2009.09.016, 2009.

Archibald, A. T., Cooke, M. C., Utembe, S. R., Shallcross, D. E., Derwent, R. G., Jenkin, M. E.: Impacts of mechanistic changes on HO$_x$ formation and recycling in the oxidation of isoprene, Atmos. Chem. Phys., 10, 8097–8118, doi:10.5194/acp-10-8097-2010, 2010.

Atkinson, R., Baulch, D. L., Cox, R. A., Crowley, J. N., Hampson, R. F., Hynes, R. G., Jenkin, M. E., Rossi, M. J., Troe, J.: Evaluated kinetic and photochemical data for atmospheric chemistry: Volume I – gas phase reactions of O$_x$, HO$_x$, NO$_x$

and SO$_x$ species, Atmos. Chem. Phys., 4, 1461–1738, 2004, http://www.atmos-chem-phys.net/4/1461/2004/.

Atkinson, R., Baulch, D. L., Cox, R. A., Crowley, J. N., Hampson, R. F., Hynes, R. G., Jenkin, M. E., Rossi, M. J., Troe, J., and IUPAC Subcommittee: Evaluated kinetic and photochemical data for atmospheric chemistry: Volume II - gas phase reactions of organic species, Atmos. Chem. Phys., 6, 3625–4055, doi:10.5194/acp-6-3625-2006, 2006.

Brasseur, G. P., Hauglustaine, D. A., Walters, S., Rasch, P. J., Müller, J.-F., Granier, C., and Tie, X. X.: MOZART, a global chemical transport model for ozone and related chemical tracers, 1. Model description, J. Geophys. Res., 103(D21), 28265–28290, 1998.

Butler, T. M., Taraborrelli, D., Brühl, C., Fischer, H., Harder, H., Martinez, M., Williams, J., Lawrence, M. G., and Lelieveld, J.: Improved simulation of isoprene oxidation chemistry with the ECHAM5/MESSy chemistry-climate model: lessons from the GABRIEL airborne field campaign, Atmos. Chem. Phys., 8, 4529–4546, doi:10.5194/acp-8-4529-2008, 2008.

Carslaw, N., Creasey, D. J., Harrison, D., Heard, D. E., Hunter, M. C. , Jacobs, P. J., Jenkin, M.E., Lee, J.D., Lewis, A. C. , Pilling, M.J., Saunders, S. M., and Seakins, P.W.: OH and HO$_2$ radical chemistry in a forested region of north-western Greece, Atmos. Environ., 35, 4725–4737, 2001.

Commane, R., Floquet, C. F. A., Ingham, T., Stone, D., Evans, M. J., Heard, D. E.: Observations of OH and HO$_2$ radicals over West Africa, Atmos. Chem. Phys., 10, 8783–8801, doi:10.5194/acp-10-8783-2010, 2010.

Crawford, J., Davis, D., Olson, J., et al.: Assessment of upper tropospheric HO$_x$ source over the tropical Pacific based on NASA GTE/PEM data: Net affect on HO$_x$ and other photochemical parameters, J. Geophys. Res., 104, 16, 255–16, 273, 1999.

Da Silva, G., Graham, C., and Wang, A.-F.: Unimolecular β-Hydroxyperoxy Radical Decomposition with OH Recycling in the Photochemical Oxidation of Isoprene, Environ. Sci. Technol., 44, 250–256, 2010.

Di Carlo, P., Brune, W. H., Martinez, M., Harder, H., Lesher, R., Ren, X. Thornberry, T., Carroll, M. A., Young, V., Shepson, P. B., Riemer, D., Apel, E., and Campbell, C.: Missing OH Reactivity in a Forest: Evidence for Unknown Reactive Biogenic VOCs, Science, 304, 722–725, 2004.

Dillon, T. J. and Crowley, J. N.: Direct detection of OH formation in the reactions of HO$_2$ with CH$_3$C(O)O$_2$ and other substituted peroxy radicals, Atmos. Chem. Phys., 8, 4877–4889, doi:10.5194/acp-8-4877-2008, 2008.

Dlugi, R., Berger, M., Zelger, M., Hofzumahaus, A., Siese, M., Holland, F., Wisthaler, A., Grabmer, W., Hansel, A., Koppmann, R., Kramm, G., Mllmann-Coers, M., and Knaps, A.: Turbulent exchange and segregation of HOx radicals and volatile organic compounds above a deciduous forest, Atmos. Chem. Phys., 10, 6215–6235, doi:10.5194/acp-10-6215-2010, 2010.

Eerdekens, G., Ganzeveld, L., Vilà-Guerau de Arellano, J., Klüpfel, T., Sinha, V., Yassaa, N., Williams, J., Harder, H., Kubistin, D., Martinez, M., and Lelieveld, J.: Flux estimates of isoprene, methanol and acetone from airborne PTR-MS measurements over the tropical rainforest during the GABRIEL 2005 campaign, Atmos. Chem. Phys., 9, 4207–4227, doi:10.5194/acp-9-4207-2009, 2009.

Eisele, F. L., Mount, G. H., Fehsenfeld, F. C., Harder, J., Marovich, E., Parrish, D. D., Roberts, J., and Trainer, M.: Intercomparison of tropospheric OH and ancillary trace gas measurements at Fritz Peak Observatory, Colorado, J. Geophys. Res., 99, 18, 605–626, 1994.

Fehsenfeld, F., Calvert, J., Fall, R., Goldan, P., Guenther, A. B., Hewitt, C. N., Lamb, B., Liu, S., Trainer, M., Westberg, H., and Zimmermann, P.: Emissions of volatile organic compounds from vegetation and the implications for atmospheric chemistry, Global Biogeochem. Cy., 6, 389–430, 1992.

Frost, G. J., Ellison, G. B., and Vaida, V.: Organic Peroxyl Radical Photolysis in the Near-Infrared: Effects on Tropospheric Chemistry J. Phys. Chem. A, 103, 10169–10178, 1999.

Fuentes, J. D., Lerdau, M., Atkinson, R., et al.: Biogenic hydrocarbons in the atmospheric boundary layer: A review, B. Am. Meteorol. Soc., 81(7),1537–1575, 2000.

Fuchs, H., Brauers, T., Dorn, H.-P., Harder, H., Häseler, R., Hofzumahaus, A., Holland, F., Kanaya, Y., Kajii, Y., Kubistin, D., Lou, S., Martinez, M., Miyamoto, K., Nishida, S., Rudolf, M., Schlosser, E., Wahner, A., Yoshino, A., and Schurath, U.: Technical Note: Formal blind intercomparison of HO$_2$ measurements in the atmosphere simulation chamber SAPHIR during the HOxComp campaign, Atmos. Chem. Phys. Discuss., 10, 21189–21235, doi:10.5194/acpd-10-21189-2010, 2010.

Ganzeveld, L., Eerdekens, G., Feig, G., Fischer, H., Harder, H., Königstedt, R., Kubistin, D., Martinez, M., Meixner, F. X., Scheeren, H. A., Sinha, V., Taraborrelli, D., Williams, J., Vil-Guerau de Arellano, J., and Lelieveld, J.: Surface and boundary layer exchanges of volatile organic compounds, nitrogen oxides and ozone during the GABRIEL campaign, Atmos. Chem. Phys., 8, 6223–6243, doi:10.5194/acp-8-6223-2008, 2008.

Gierczak, T., Burkholder, J. B., Talukdar, R. K., Mellouki, A., Barone, S. B., and Ravishankara, A. R.: Atmospheric fate of methyl vinyl ketone and methacrolein, J. Photoch. Photobio. A, 110, 1–10, 1997.

Goldstein, A. H., McKay, M., Kurpius, M. R., Schade, G. W., Lee, A., Holzinger, R., Rasmussen, R. A.: Forest thinning experiment confirms ozone deposition to forest canopy is dominated by reaction with biogenic VOCs, Geophys. Res. Lett., 31, L22106, doi:10.1029/2004GL021259, 2004.

Granier, C., Pétron, G., Müller, J.-F., and Brasseur, G.: The impact of natural and anthropogenic hydrocarbons on the tropospheric budget of carbon monoxide, Atmos. Environ., 34, 5255–5270, 2000.

Guenther, A. B., Hewitt, G. N., Erickson, D., et al.: A global model of natural volatile organic compound emissions, J. Geophys. Res., 100(D5), 8873–8892, 1995.

Hasson, A. S., Tyndall, G. S., and Orlando, J. J.: A product yield study of the reaction of HO2 radicals with Ethyl Peroxy (C$_2$H$_5$O$_2$), Acetyl Peroxy (CH$_3$C(O)O$_2$), and Acetonyl Peroxy (CH$_3$C(O)CH$_2$O$_2$) Radicals, J.Phys. Chem. A, 108, 5979–5989, 2004.

Heard, D. E. and Pilling, M. J.: Measurement of OH and HO$_2$ in the Troposphere, Chem. Rev., 103, 5163–5198, 2003.

Hewitt, C. N., Lee, J. D., MacKenzie, A. R., Barkley, M. P., Carslaw, N., Carver, G. D., Chappell, N. A., Coe, H., Collier, C., Commane, R., Davies, F., Davison, B., DiCarlo, P., Di Marco, C. F., Dorsey, J. R., Edwards, P. M., Evans, M. J.,

Fowler, D., Furneaux, K. L., Gallagher, M., Guenther, A., Heard, D. E., Helfter, C., Hopkins, J., Ingham, T., Irwin, M., Jones, C., Karunaharan, A., Langford, B., Lewis, A. C., Lim, S. F., MacDonald, S. M., Mahajan, A. S., Malpass, S., McFiggans, G., Mills, G., Misztal, P., Moller, S., Monks, P. S., Nemitz, E., Nicolas-Perea, V., Oetjen, H., Oram, D. E., Palmer, P. I., Phillips, G. J., Pike, R., Plane, J. M. C., Pugh, T., Pyle, J. A., Reeves, C. E., Robinson, N. H., Stewart, D., Stone, D., Whalley, L. K., and Yin, X.: Overview: oxidant and particle photochemical processes above a south-east Asian tropical rainforest (the OP3 project): introduction, rationale, location characteristics and tools, Atmos. Chem. Phys., 10, 169–199, doi:10.5194/acp-10-169-2010, 2010.

Hofzumahaus, A., Rohrer, F., Lu, K., Bohn, B., Brauers, T., Chang, C., Fuchs, H., Holland, F., Kita, K., Kondo, Y., Li, X., Lou, S., Shao, M., Zeng, L., Wahner, A., and Zhang Y.: Amplified Trace Gas Removal in the Troposphere, Science, 324, 1702–1704, 2009.

Jackson, A. V. and Hewitt, C. N.: Atmosphere Hydrogen Peroxide and Organic Hydorperoxides: A Review, Critical Reviews in Environmental Science and Technolology, 29(2), 175–228, 1999.

Jenkin, M. E. and Hayman, G. D.: Kinetics of Reactions of Primary, Secondary and Tertiary β-Hydroxy Peroxyl Radicals, Application to Isoprene Degradation, J. Chem. Soc. Faraday Trans., 91(13), 1911–1922, 1995.

Jenkin, M. E., Saunders, S. M., and Pilling, M. J.: The tropospheric degradation of volatile organic compounds: a protocol for mechanism development, Atmos. Environ. 31, 81–104, 1997.

Jenkin, M. E., Hurley, M. D., and Wallington, T. J.: Investigation of the radical product channel of the $CH_3COO_2 + HO_2$ reaction in the gas phase, Phys. Chem. Chem. Phys. 9, 3149–3162, 2007.

Jöckel, P., Tost, H., Pozzer, A., Brühl, C., Buchholz, J., Ganzeveld, L., Hoor, P., Kerkweg, A., Lawrence, M. G., Sander, R., Steil, B., Stiller, G., Tanarhte, M., Taraborrelli, D., van Aardenne, J., and Lelieveld, J.: The atmospheric chemistry general circulation model ECHAM5/MESSy1: consistent simulation of ozone from the surface to the mesosphere, Atmos. Chem. Phys., 6, 5067–5104, doi:10.5194/acp-6-5067-2006, 2006.

Karl, T., Guenther, A., Yokelson, R. J., Greenberg, J., Potosnak, M., Blake, D. R., Artaxo, P.: The tropical forest and fire emissions experiment: Emission, chemistry and transport of biogenic volatile organic compounds in the lower atmosphere over Amazonia, J. Geophys. Res., 112, D18302, doi:10.1029/2007JD008539, 2007.

Kesselmeier, J. and Staudt, M.: Biogenic volatile organic compounds (VOC): An overview on emission, physiology and ecology, J. Atmos. Chem., 33, 23–88, 1999.

Kleindienst, T. E., Lewandowski, M., Offenberg, J. H., Jaoui, M., and Edney, E. O.: The formation of secondary organic aerosol from the isoprene + OH reaction in the absence of NO$_x$, Atmos. Chem. Phys., 9, 6541–6558, doi:10.5194/acp-9-6541-2009, 2009.

Krol, M. C., Molemaker, M. J., and Vilà Guerau de Arellano, J.: Effects of turbulence and heterogeneous emissions on photochemically active species in the convective boundary layer, J. Geophys. Res., 105(D5), 6871–6884, 2000.

Von Kuhlmann, R., Lawrence, M. G., and Crutzen, P. J.: A model for studies of tropospheric ozone and nonmethane hydrocarbons: Model descriptions and ozone results, J. Geophys. Res., 108(D9),

4294 pp., 2003.

von Kuhlmann, R., Lawrence, M. G., Pöschl, U., and Crutzen, P. J.: Sensitivities in global scale modeling of isoprene, Atmos. Chem. Phys., 4, 1–17, doi:10.5194/acp-4-1-2004, 2004.

Kuhn, U., Andreae, M. O., Ammann, C., Araújo, A. C., Brancaleoni, E., Ciccioli, P., Dindorf, T., Frattoni, M., Gatti, L. V., Ganzeveld, L., Kruijt, B., Lelieveld, J., Lloyd, J., Meixner, F. X., Nobre, A. D., Pöschl, U., Spirig, C., Stefani, P., Thielmann, A., Valentini, R., and Kesselmeier, J.: Isoprene and monoterpene fluxes from Central Amazonian rainforest inferred from tower-based and airborne measurements, and implications on the atmospheric chemistry and the local carbon budget, Atmos. Chem. Phys., 7, 2855–2879, doi:10.5194/acp-7-2855-2007, 2007.

Lelieveld, J., Peters, V., Dentener, F. J., and Krol, M.: Stability of tropospheric hydroxyl chemistry, J. Geophys. Res. 107, 4715 pp., doi:10.1029/2002JD002272, 2002.

Lelieveld, J., Butler, T. M., Crowley, J., Dillon, T., Fischer, H., Ganzeveld, L., Harder, H., Lawrence, M. G., Martinez, M., Taraborrelli, D., and Williams, J.: Atmospheric oxidation capacity sustained by a tropical forest, Nature, 452, 737–740, 2008.

Levy II, H.: Normal atmosphere: Large radical and formaldehyde concentrations predicted, Science, 173, 141–143, 1971.

Logan, J. A., Prather, M. J., Wofsy, S. C., and McElroy, M. B.: Tropospheric chemistry: A global perspective, J. Geophys. Res., 86, 7210–7254, 1981.

Madronich, S. and Flocke, S.: The role of solar radiation in atmospheric chemistry, in: Handbook of Environmental Chemistry, edited by: Boule, P., 1–26, Springer, New York, USA, 1998.

Martin, S. T., Andreae, M. O., Artaxo, P., Baumgardner, D., Chen, Q., Goldstein, A. H., Guenther, A., Heald, C. L., Mayol-Bracero, O. L., McMurry, P. H., Pauliquevis, T., Pöschl, U., Prather, K. A., Roberts, G. C., Saleska, S. R., Silva Dias, M. A., Spracklen, D. V., Swietlicki, E., and Trebs, I.: Sources and properties of amazonian sources and properties of amazonian aerosol particles, Rev. Geophys., 48, RG2002, 42 pp., 2010.

Martinez, M., Harder, H., Kubistin, D., Rudolf, M., Bozem, H., Eerdekens, G., Fischer, H., Klüpfel, T., Gurk, C., Königsstedt, R., Parchatka, U., Schiller, C. L., Stickler, A., Williams, J., and Lelieveld, J.: Hydroxyl radicals in the tropical troposphere over the Suriname rainforest: airborne measurements, Atmos. Chem. Phys., 10, 3759–3773, doi:10.5194/acp-10-3759-2010, 2010.

Paulot, F., Crounse, J. D., Kjaergaard, H. G., Kürten, A., Clair, J. M. St., Seinfeld, J. H., and Wennberg, P. O.: Unexpected Epoxide Formation in the Gas-Phase Photooxidation of Isoprene, Science, 325(5941), 730–733, 2009.

Paulson, S. E., Flagan, R. C., and Seinfeld, J. H.: Atmospheric photo-oxidation of isoprene: part I: the hydroxyl radical and ground state atomic oxygen reactions, Int. J. Chem. Kinet., 24, 79–101, 1992.

Peeters, J., Nguyenz, T. L., and Vereecken, L.: HO$_x$ radical regeneration in the oxidation of isoprene, Phys. Chem. Chem. Phys., 11, 5935–5939, 2009.

Pinho, P. G., Pio, C. A., and Jenkin, M. E.: Evaluation of isoprene degradation in the detailed tropospheric chemical mechanism, MCM v3, using environmental chamber data, Atmos. Environ., 39, 1303–1322, 2005.

Pöschl, U., Von Kuhlmann, R., Poisson, N., and Crutzen, P. J.: Development and intercomparison of condensed isoprene oxidation mechanisms for global atmospheric modeling, J. Atmos. Chem., 37, 29–52, 2000.

Poisson, N., Kanakidou, M., and Crutzen, P. J.: Impact of Non-Methane Hydrocarbons on Tropospheric Chemistry and the Oxidizing Power of the Gobal Troposphere: 3-Dimensional Modelling Results, J. Atmos. Chem., 36, 157–230, 2000.

Pugh, T. A. M., MacKenzie, A. R., Hewitt, C. N., Langford, B., Edwards, P. M., Furneaux, K. L., Heard, D. E., Hopkins, J. R., Jones, C. E., Karunaharan, A., Lee, J., Mills, G., Misztal, P., Moller, S., Monks, P. S., and Whalley, L. K.: Simulating atmospheric composition over a South-East Asian tropical rainforest: performance of a chemistry box model, Atmos. Chem. Phys., 10, 279–298, doi:10.5194/acp-10-279-2010, 2010.

Pugh, T. A. M., MacKenzie, A. R., Langford, B., Nemitz, E., Misztal, P. K., and Hewitt, C. N.: The influence of small-scale variations in isoprene concentrations on atmospheric chemistry over a tropical rainforest, Atmos. Chem. Phys. Discuss., 10, 18197–18234, doi:10.5194/acpd-10-18197-2010, 2010.

Ren, X., Olson, J. R., Crawford, J. H., Brune, W. H., Mao, J., Long, R. B., Chen, Z., Chen, G., Avery, M. A., Sachse, G. W., Barrick, J. D., Diskin, G. S., Huey, L. G., Fried, A., Cohen, R. C., Heikes, B., Wennberg, P., Singh, H. B., Blake, D. R., Shetter, R. E.: HO$_x$ chemistry during INTEX-A 2004: Observation, model calculation, and comparison with previous studies, J. Geophys. Res., 113, D05310, doi:10.1029/2007JD009166, 2008.

Sander, R., Kerkweg, A., Jöckel, P., and Lelieveld, J.: Technical note: The new comprehensive atmospheric chemistry module MECCA, Atmos. Chem. Phys., 5, 445–450, doi:10.5194/acp-5-445-2005, 2005.

Sander, S. P., Finlayson-Pitts, B. J., Friedl, R. R., Golden, D. M., Huie, Kolb, C. E., R. E., Kurylo, M. J., Molina, M. J., Moortgat, G. K., Orkin, V. L., Ravishankara, A. R.: Chemical Kinetics and Photochemical Data for Use in Atmospheric Studies, Evaluation Number 14, JPL Publication 02–25, Jet Propulsion Laboratory, Pasadena, California, 2006.

Sander, S. P., Friedl, R. R., Golden, D. M., Kurylo, M. J., Moortgat, G. K., Wine, P. H., Ravishankara, A. R., Kolb, C. E., Molina, M. J., Finlayson-Pitts, B. J., Huie, R. E., and Orkin, V. L.: Chemical Kinetics and Photochemical Data for Use in Atmospheric Studies, Evaluation Number 15, JPL Publication 06–2, NASA Jet Propulsion Laboratory, Pasadena, California, 2006.

Saunders, S. M., Jenkin, M. E., Derwent, R. G., and Pilling, M. J.: World wide web site of a master chemical mechanism (MCM) for use in tropospheric chemistry models, Atmos. Environ., 31, p. 1249, http://www.chem.leeds.ac.uk/Atmospheric/MCM, 1997.

Saunders, S. M., Jenkin, M. E., Derwent, R. G., Pilling, M. J.: Protocol for the development of the Master Chemical Mechanism, MCM v3 (Part A): tropospheric degradation of non-aromatic volatile organic compounds, Atmos. Chem. Phys., 3, 161-180, 2003,
http://www.atmos-chem-phys.net/3/161/2003/.

Saunois, M., Reeves, C. E., Mari, C. H., Murphy, J. G., Stewart, D. J., Mills, G. P., Oram, D. E., Purvis, R. M.: Factors controlling the distribution of ozone in the West African lower troposphere during the AMMA (African Monsoon Multidisciplinary Analysis) wet season campaign, Atmos. Chem. Phys., 9, 6135-6155, 2009,
http://www.atmos-chem-phys.net/9/6135/2009/.

Schlosser, E., Brauers, T., Dorn, H.-P., Fuchs, H., Hseler, R., Hofzumahaus, A., Holland, F., Wahner, A., Kanaya, Y., Kajii, Y., Miyamoto, K., Nishida, S., Watanabe, K., Yoshino, A., Kubistin, D., Martinez, M., Rudolf, M., Harder, H., Berresheim, H., Elste, T., Plass-Dlmer, C., Stange, G., Schurath, U.: Technical Note: Formal blind intercomparison of OH measurements: results from the international campaign HOxComp, Atmos. Chem. Phys., 9, 7923–7948, doi:10.5194/acp-9-7923-2009, 2009.

Schmidt, U.: Molecular hydrogen in the atmosphere, Tellus, 26, 78-90, 1974.

Schmidt, U.: The latitudinal and vertical distribution of molecular hydrogen in the troposphere, J. Geophys. Res., 83, 941-946, 1978.

Sinha, V., Williams, J., Crowley, J. N., and Lelieveld, J.: The Comparative Reactivity Method - a new tool to measure total OH Reactivity in ambient air, Atmos. Chem. Phys., 8, 2213–2227, 2008,
http://www.atmos-chem-phys.net/8/2213/2008/.

Stavrakou, T., Peeters, J., and Müller, J.-F.: Improved global modelling of HOx recycling in isoprene oxidation: evaluation against the GABRIEL and INTEX-A aircraft campaign measurements, Atmos. Chem. Phys. Discuss., 10, 16551–16588, doi:10.5194/acpd-10-16551-2010, 2010.

Stickler, A., Fischer, H., Bozem, H., Gurk, C., Schiller, C., Martinez-Harder, M., Kubistin, D., Harder, H., Williams, J., Eerdekens, G., Yassaa, N., Ganzeveld, L., Sander, R., and Lelieveld, J.: Chemistry, transport and dry deposition of trace gases in the boundary layer over the tropical Atlantic Ocean and the Guyanas during the GABRIEL field campaign, Atmos. Chem. Phys., 7, 3933–3956, doi:10.5194/acp-7-3933-2007, 2007.

Stone, D., Evans, M. J., Commane, R., Ingham, T., Floquet, C. F. A., McQuaid, J. B., Brookes, D. M., Monks, P. S., Purvis, R., Hamilton, J. F., Hopkins, J., Lee, J., Lewis, A. C., Stewart, D., Murphy, J. G., Mills, G., Oram, D., Reeves, C. E., and Heard, D. E.: HO$_x$ observations over West Africa during AMMA: impact of isoprene and NO$_x$, Atmos. Chem. Phys., 10, 9415–9429, doi:10.5194/acp-10-9415-2010, 2010.

Tan., D., Faloona, I., Simpas, J. B., Brune, W., Shepson, P. B., Couch, T. L., Summer, A. L., Carroll, M. A., Thornberry, T., Apel, E., Riemer, D., and Stockwell, W.: HO$_x$ budgets in a deciduous forest: Results from the PROPHET summer 1998 campaign, J. Geophys. Res. 106, 24407–24427, 2001.

Taraborrelli, D., Lawrence, M. G., Butler, T. M., Sander, R., and Lelieveld, J.: Mainz Isoprene Mechanism 2 (MIM2): an isoprene oxidation mechanism for regional and global atmospheric modelling, Atmos. Chem. Phys., 9, 2751–2777, doi:10.5194/acp-9-2751-2009, 2009.

Thornton, J. A., Wooldridge, P. J., Cohen, R. C., Martinez, M., Harder, H., Brune, W. H., Williams, E. J., Roberts, J. M., Fehsenfeld, F. C., Hall, S. R., Shetter, R. E., Wert, B. P., and Fried, A.: Ozone production rates as a function of NO$_x$ abundances and HO$_x$ production rates in the Nashville urban plume, J. Geophys. Res., 107, 4146(D12), 4146, doi:10.1029/2001JD000932, 2002.

Vaghjiani, G. L. and Ravishankara, A. R.: Absorption cross sections

of CH$_3$OOH, H$_2$O$_2$ and D$_2$O$_2$ vapors between 210 nm and 365 nm at 297 K, J. Geophys. Res., 94, 3487–3492, 1989.

Wang, Y., Jacob, D. J., and Logan, J. A.: Global simulations of tropospheric O$_3$ - NO$_x$ - hydrocarbon chemistry. 3 Origin of tropospheric ozone effects of non-methane hydrocarbons, J. Geophys. Res., 103, 10757–10767, 1998.

Warneke, C., Holzinger, R., Hansel, A., Jordan, A., Lindinger, W., Pöschl, U., Williams, J., Hoor, P., Fischer, H., Crutzen, P. J., Scheeren, H. A., and Lelieveld, J.: Isoprene and Its Oxidation Products Methyl Vinyl Ketone, Methacrolein, and Isoprene Related Peroxides Measured Online over the Tropical Rain Forest of Suriname in March 1998, J. Atmos. Chem., 38, 167–185, 2001.

Whalley, L. K., Furneaux, K. L., Goddard, A., Lee, J. D., Mahajan, A., Oetjen, H., Read, K. A., Kaaden, N., Carpenter, L. J., Lewis, A. C., Plane, J. M. C., Saltzman, E. S., Wiedensohler, A., and Heard, D. E.: The chemistry of OH and HO2 radicals in the boundary layer over the tropical Atlantic Ocean, Atmos. Chem. Phys., 10, 1555–1576, doi:10.5194/acp-10-1555-2010, 2010.

Williams, J., Yassaa, N., Bartenbach, S., and Lelieveld, J.: Mirror image hydrocarbons from Tropical and Boreal forests, Atmos. Chem. Phys., 7, 973–980, doi:10.5194/acp-7-973-2007, 2007.

Zimmermann, P. R., Greenberg, J. P., and Westberg, C. E.: Measurements of atmospheric hydrocarbons and biogenic emission fluxes in the Amazon boundary layer, J. Geophys. Res., 93, 1407–1416, 1988.